REPORT DOCUMENTATION PAGE

AD-A199 962		1b. RESTRICTIVE MARKINGS

1b. RESTRICTIVE MARKINGS

3. DISTRIBUTION / AVAILABILITY OF REPORT
Approved for public release,
distribution unlimited

LE

4. PERFORMING ORGANIZATION REPORT NUMBER(S)
UTSI Report 88-06

5. MONITORING ORGANIZATION REPORT NUMBER(S)
AFOSR·TR· 88-0937

6a. NAME OF PERFORMING ORGANIZATION The University of Tennessee Space Institute	6b. OFFICE SYMBOL (If applicable) UTSI	7a. NAME OF MONITORING ORGANIZATION AFOSR/ Bolling AFB, DC 20332

6c. ADDRESS (City, State, and ZIP Code) Gas Dynamics Division Tullahoma, TN 37388	7b. ADDRESS (City, State, and ZIP Code) AFOSR/ Bolling AFB, DC 20332

8a. NAME OF FUNDING / SPONSORING ORGANIZATION Office of Scientific Research	8b. OFFICE SYMBOL (If applicable) AFOSR/NA	9. PROCUREMENT INSTRUMENT IDENTIFICATION NUMBER AFOSR 86-0155

8c. ADDRESS (City, State, and ZIP Code)
USAF OSR
Bolling Air Force Base
Washington, D.C. 20332-6448

10. SOURCE OF FUNDING NUMBERS

PROGRAM ELEMENT NO.	PROJECT NO.	TASK NO.	WORK UNIT ACCESSION NO.
61102F	2307	A1	

11. TITLE (Include Security Classification)
Phenomena of Discrete Wingtip Jets

12. PERSONAL AUTHOR(S)
J. M. Wu, A. D. Vakili, Z. Shi and J. D. Mo

13a. TYPE OF REPORT Final Technical Report	13b. TIME COVERED FROM May 86 TO Aug.88	14. DATE OF REPORT (Year, Month, Day) August 1988	15. PAGE COUNT 55

16. SUPPLEMENTARY NOTATION

17.	COSATI CODES		18. SUBJECT TERMS (Continue on reverse if necessary and identify by block number)
FIELD	GROUP	SUB-GROUP	wing performance, lift augmentation, discrete jets, wingtip jet blowing, asymmetric jet, jet in crossflow, tip blowing, vortex control, jet vortices, flow visualizations, jet application, wingtip vortex wake, tip vortex dispersion,

19. ABSTRACT (Continue on reverse if necessary and identify by block number)

Detail flow phenomena of discrete wingtip jets blowing from a rectangular wing with squared edges and round tips are investigated in the water- and wind-tunnel experiments. Phenomena on a single asymmetric jet blowing from a flat-plate in crossflow were incorporated into the present wingtip jet study. The local flow field perturbation introduced by the tip jet blowing closely resembles that of the asymmetric jet from the flat-plate. The wingtip jet has influenced the global surface pressure distribution over the wing and improved the lift loading. A simple mathematical model is developed for practical calculation of wing loading.

DTIC
ELECTE
OCT 05 1988
S   E   D

20. DISTRIBUTION / AVAILABILITY OF ABSTRACT ☒ UNCLASSIFIED/UNLIMITED ☒ SAME AS RPT ☐ DTIC USERS	21. ABSTRACT SECURITY CLASSIFICATION
22a. NAME OF RESPONSIBLE INDIVIDUAL L. SAKELL	22b. TELEPHONE (Include Area Code) 202 767 4935	22c. OFFICE SYMBOL AFOSR/NA

DD FORM 1473, 84 MAR
83 APR edition may be used until exhausted.
All other editions are obsolete.

SECURITY CLASSIFICATION OF THIS PAGE

88 10 5 181

AFOSR·TR· 88-0937

Fl/AL Report

~~REVIEW COPY~~

Investigation of

Phenomena of Discrete Wingtip Jets

by

J. M. Wu, A. D. Vakili, Z. Shi, and J. D. Mo

The University of Tennessee Space Institute

Tullahoma, Tennessee 37388

August 1988

UTSI Report 88-06

Accession For	
NTIS GRA&I	☒
DTIC TAB	☐
Unannounced	☐
Justification	
By	
Distribution/	
Availability Codes	
Dist	Avail and/or Special
A-1	

QUALITY INSPECTED 4

TABLE OF CONTENTS

SUMMARY

Detail flow phenomena of discrete wingtip jets blowing from a rectangular wing with squared edges and rounded tips were investigated in the water and wind tunnel experiments. Previously observed phenomena on a single asymmetric jet blowing vertically from a flat plate in crossflow were incorporated into the present study. It was found that the local flowfield perturbation introduced by the wingtip jet blowing closely resembles that of the asymmetric jet blowing from the flat plate. The wingtip jet blowing influenced the global surface pressure distribution over the wing and improved the lift loading. It was reconfirmed that the wingtip jets can be used to disperse the tip vortex. The tip-wake flow the jet blowing contains multi-vortices. A simple mathematical model predicts the trends of various parameters involved reasonably well and may be used for practical calculation.

1

I. INTRODUCTION

Flow in the tip region of any lifting wing is complex and three-dimensional. The details of the flow structure in this region has a large influence on the performance of the wing. Even since it was recognized that the three-dimensional wing produced an induced drag, many efforts have been made to reduce this drag and increase the lift/drag ratio by modifying the wing configuration including its tip. Among numerous work done on this subject, Ayers and Wilde [1] started the idea of improving the wing performance by using spanwise blowing from the tips in 1956. Since then, many works have been done both experimentally [2-15] and theoretically [16-18] in this area.

Although it has become known and established that the wingtip blowing can improve the wing performance, the detail flow structure and the physical mechanism of it are still not clear. This is because of the wingtip flowfield with jet blowing is so complex. The tip flowfield is affected by the combination of free stream velocity, angle of attack and the momentum of blowing jet. It is unsteady, turbulent and contains many vortices. All these make the theoretical and computational studies of the wingtip flowfield become tremendously difficult.

For this reason, Wu, Vakili, and Yu [19-21] initiated the basic investigation of the detail features associated with a single non-symmetric jet in crossflow. It was found that non-symmetric jet in crossflow provides a complex interacting flowfield which has a kidney shaped jet cross-section and contains many vortices. Both the shape and the vortices vary significantly with variations of the jet and the crossflow conditions. Among many vortices produced in this interaction, four major vortices were identified. They found that under certain flow conditions, shedding vortices appear and disappear periodically. Figure 1.1 illustrates a typical flow pattern of non-symmetric jet in crossflow. This cross-sectional view was made visible by using laser-fluorescence visualization technique. The kidney shape jet vortices and several other vortices are clearly shown in the picture.

Lee, Tavella, and Wood [11, 12, 15] have investigated the wingtip jet blowing. They studied the wake flow of a wing which incorporates blowing from a long, thin slit at the
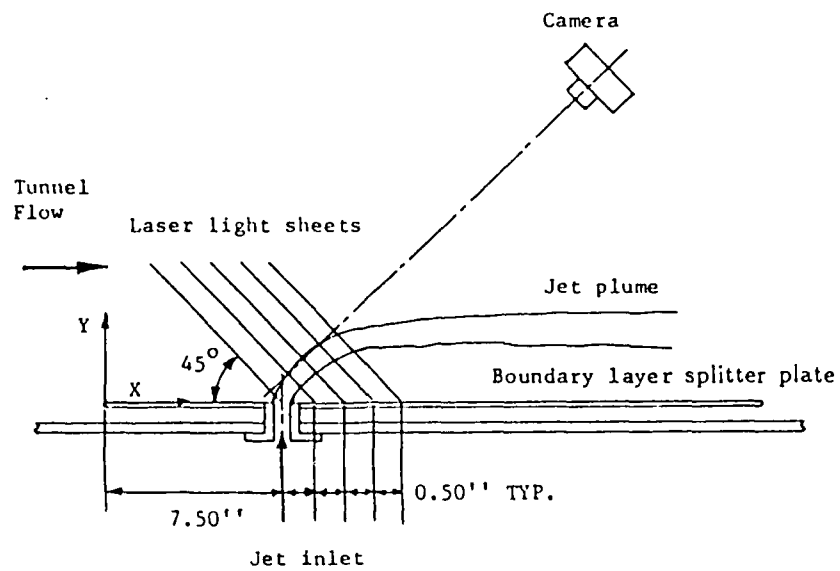
2

Camera

Tunnel
Flow

Laser light sheets

Jet plume

Y

45°

X

Boundary layer splitter plate

0.50'' TYP.

7.50''

Jet inlet

Figure 1.1. Laser-fluorescence sectional view of a non-symmetric jet in crossflow $V_j/V_\infty = 2$, Red $= 240$ (Yu, 1987).

3

wingtip. They observed that straight lateral blowing at angle of attack greater than 2 deg, blowing creates a lateral displacement of the tip vortex without complicating the vortex structure. For other jet configurations at small angle of attack, however, the wingtip jet blowing produces secondary vortices. One of their experimental results is shown in Figure 1.2, the induced vortices appeared very clearly far downstream of the model.

The purpose of present study was to further explore the detail features of wingtip jet blowing flowfield based on knowledge acquired. The experimental works conducted were water tunnel flow visualization, surface oil flow, wing surface pressure distribution measurement and wake survey. It was attempted to find the shape and detail structure of the wingtip jet flowfield by flow visualization in water tunnel and surface oil flow in the wind tunnel. The pressure measurement and wake survey were used to study the behavior of this flowfield. Some computational studies were also done in order to modify this flowfield and optimize the best jet location.
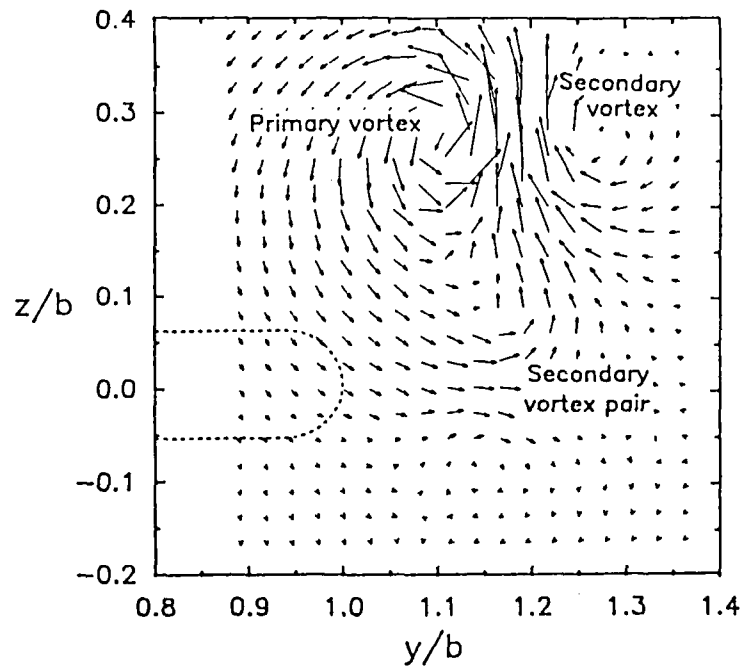
(a) velocity field by five-hole probe measurement
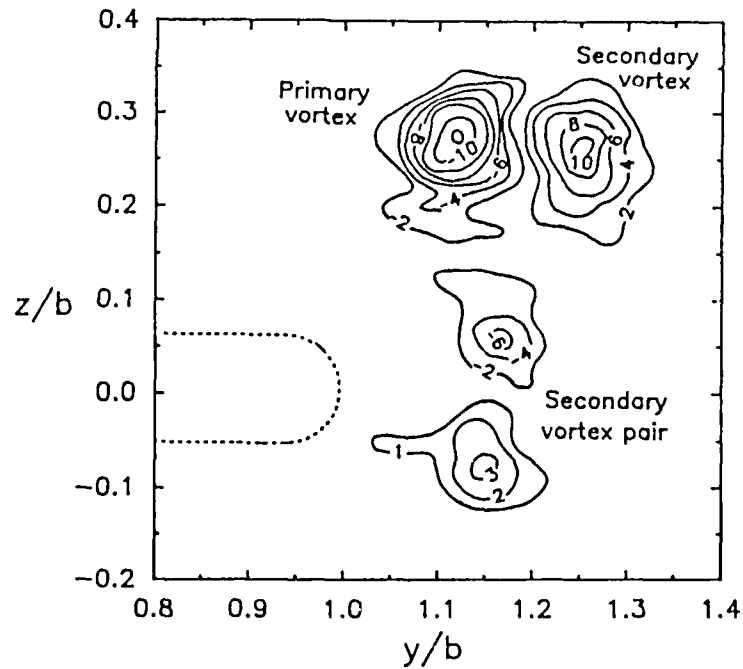
(b) volicity contours ($\zeta b / V_\infty$)

Figure 1.2. Wake flow structure for wingtip jet blowing, $\alpha = 2^o$, $C_\mu = 0.18, x/c = 2.4$ (Lee, Tavella & Wood, 1987).

5

II. WATER TUNNEL EXPERIMENT

The present investigation was undertaken to study more details of flowfield around wingtips with discretely positioned tip blowing jets. In particular, it was considered essential to identify and to study the vortex system generated by such jets. Careful observations of wingtip flow pattern were made to identify the source of vortices and their influences. This part of the study was conducted at The University of Tennessee Space Institute (UTSI) water tunnel.

Two flow visualization techniques were used in this experimental study: (a) colored dye (food color in a milk-alcohol mixture), and (b) laser induced fluorescence. The former gave the global flow pattern while the later was confined to selected cross-sections of flowfield.

2.1. WATER TUNNEL FACILITY

The UTSI water tunnel was designed to provide excellent flow quality for flow visualization studies. A detailed description of this facility can be found in the UTSI report by Collins (1982).

The water tunnel was a closed circuit continuous flow facility. It lay in a horizontal plane and was powered by a 25 cm diameter two-bladed propeller which was located at the second bend downstream of the test section. The propeller was connected to a continuously variable speed transmission which allowed the tunnel speed to be varied from 1.5 to 60 cm/sec. The fluctuations from the propeller were damped by the long return pipe leading to the stilling chamber. Test section dimensions were 30.5 cm high, 45.7 cm wide and 150 cm long (12 in x 18 in x 60 in). The test section walls were made of Plexiglas for versatility in observing and photographing the flowfield.

The tunnel was controlled from a control panel, where the propeller speed was displayed with a digital meter. This meter was calibrated against the tunnel flow velocity using a cylindrical hot-film probe.

6

2.2. DESIGN AND SET-UP OF THE EXPERIMENTAL ASSEMBLY

The wing model used in this study was an NACA 0012-64 airfoil section with semi-span of 27.1 cm and chord of 16.2 cm. The model was about 9/10 scale of the wind tunnel model. One end of the model was mounted to a shaft which extended through the side wall of the water tunnel. Model angle of attack was controlled by this shaft and measured by a counter assembly exterior to the tunnel. Wingtip jet ports were located at the tip of the wing which were at 60% of the width of the tunnel. The maximum blockage of the model was less than 10%.

Two types of wingtip were used in this study; a rectangular tip and a rounded tip. The geometry of the wingtip jets were three individual rounded end rectangular shaped jets. Figure 2.1 shows the geometry of the wing model and Table 2.1 describes the details of the tip jets used in the water tunnel investigation. The jet ports were not contoured surfaces but simple openings machined through the tip into the (water) reservoir built inside the wing.

The water to the three jets were supplied from a water line via three tubes. The flow rate in each tube was measured by a flowmeter. Various combinations of jet blowings were investigated.

Flow visualization was achieved by bleeding dye through several small holes located near the wingtip. The dye bleeding system consisted of a pressure driven dye manifold that supplies dye to the model through 1.7 mm diameter vinyl tubes. Dye could also be introduced upstream or downstream of the model through several movable dye probes. The dye used was a mixture of alcohol, milk, and commercial food color in such a composition to ensure a specific gravity equal to that of water. This technique was used successfully to unveil many of the global flow features of jets in crossflow. As the dye was continuously supplied on the surface around the jet exit, it followed the local flow which were driven by the entrainment and interaction of jets.
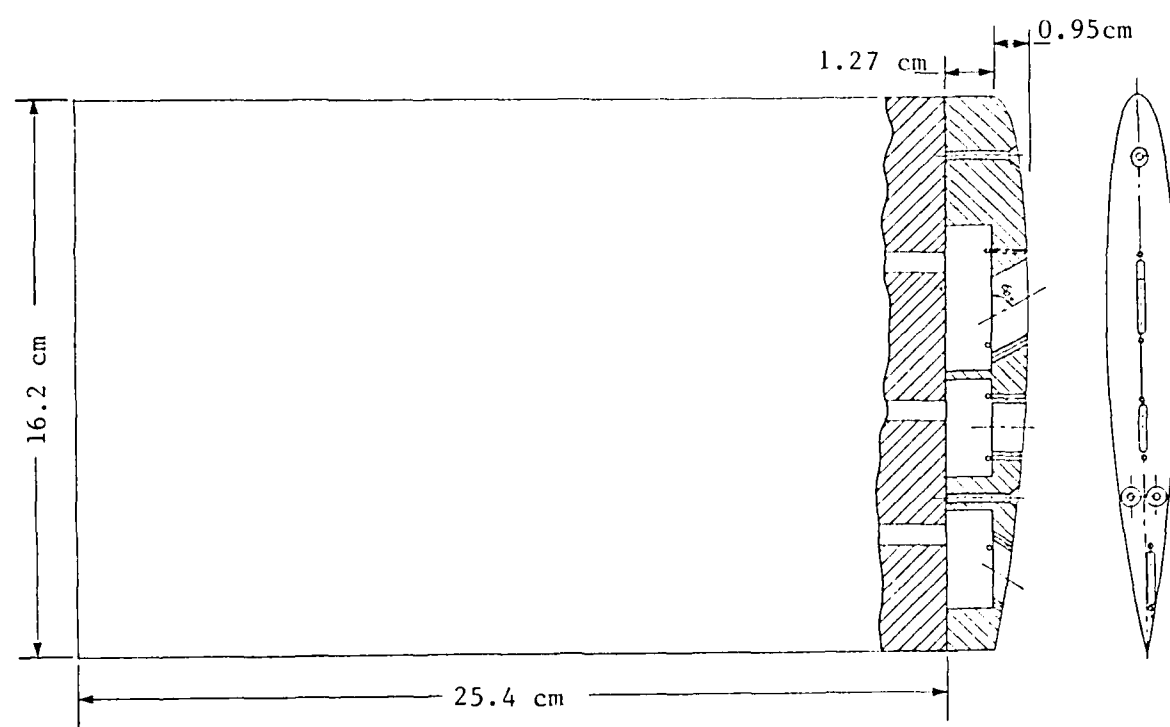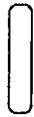
(a) drawing of the model
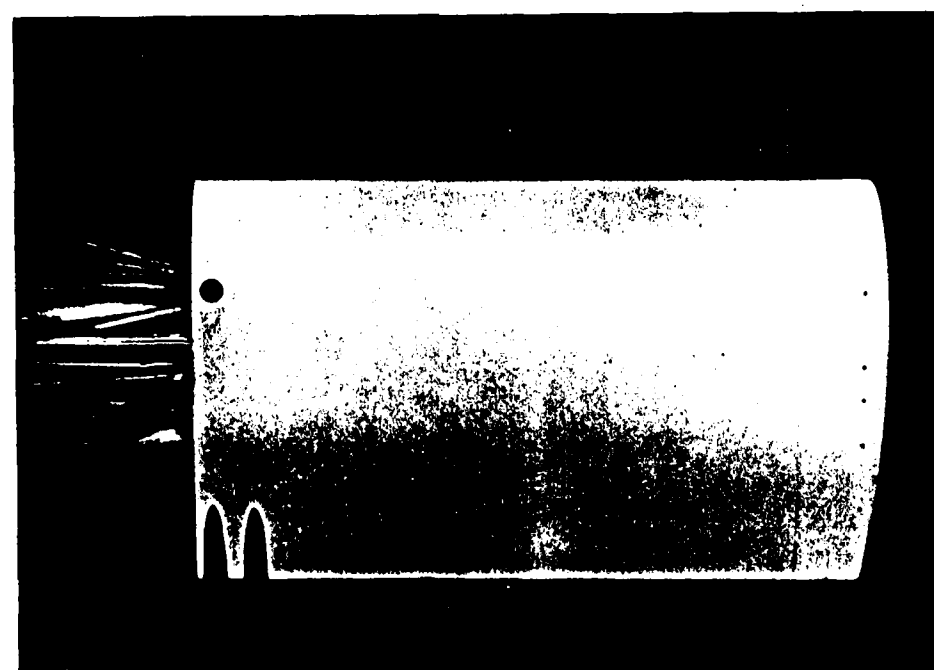
(b) photo of the model

Figure 2.1. The water tunnel model.

8

TABLE 2.1

WATER TUNNEL WING MODEL JET CONFIGURATIONS

Model	Configuration Design Parameter	Sweep Angles* δ_{j1}	δ_{j2}	δ_{j3}	Dihedral Angles** λ_1	λ_2	λ_3	Jet Shape
Rectangular Tip	Dihedral	135°	90°	45°	-30°	0°	30°	▭
Rounded Tip	Dihedral	120°	90°	60°	0°	0°	15°	▭

*Sweep angle measured along free stream direction in x-coordinate.

**Dihedral angle positive for upward blowing.

9

2.3. RESULTS AND DISCUSSION

A. VORTICES DUE TO A SINGLE JET IN CROSSFLOW

From the previous studies of jet in the crossflow [19–21], it was found that the emerging jet would bend such that its axis aligned with the local flow direction. In general, the jet in crossflow provided complex interacting flowfield which contains many vortices. These vortices varied significantly with variations of the jet and the crossflow conditions, as will be described below. Under certain specific conditions shedding vortices appeared and disappeared periodically. In Figures 2.2 through Figure 2.5, the flowfield was reconstructed schematically based on the visual observations and upon the relevant flow physics.

Under moderately high jet to freestream velocity ratio (i.e., $V_j/V_\infty \geq 2.5$) and asymmetric jet, the periodic vortex shedding was observed perpendicular to the crossflow, these were called "spin-off" vortices all rotating in the same sense, as shown in Figure 2.6 and Figure 2.7. The source for this shedding is the initial shear layer (vorticity from the boundary and from the vorticity generated on the boundary of jet exit). The pressure gradient across the jet provided a mechanism to deflect the accumulated streamwise vorticity of this shear layer. The stretching of this layer and the jet penetration into the crossflow provided the mechanism which caused shear layer instability and their breaking off to form a series of spin-off vortices. In our experiments, the spin-off vortices were observed only at jet velocity to the freestream velocity ratios higher than 2.5. They also depended on the jet port shape and orientation.

A "wake-vortex" was observed for non-symmetric jets. This vortex was lying parallel and close to the floor plate as shown in Figure 2.3 and Figure 2.8. This wake vortex was a result of non-symmetrical enhancing of one vortex by a pair of jet induced base vortices. Due to highly skewed jet vortices such induced flow phenomenon became possible. Once the spin-off vortices were present in the flowfield they became twisted and linked across the wake of the jet vortex and were found around the wake vortex near the flat plate.

The basic investigation of single jet in crossflow gave us a foundation to study the wingtip jet behavior. Our water tunnel study results showed that the complicated flowfield
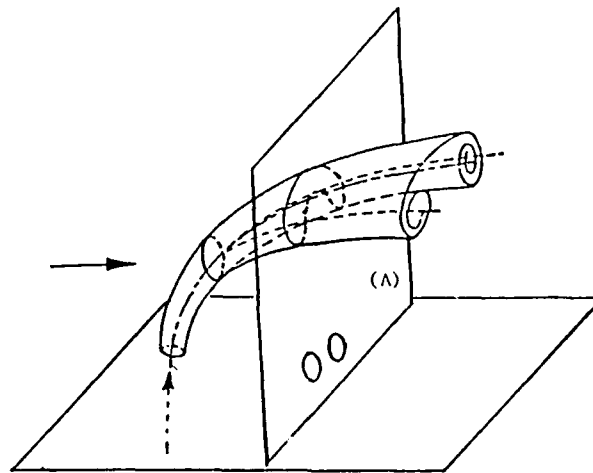
Tunnel Flow

x_3

horseshoe
vortex
(due to solid
blockage of
jet stream)

x_1

x_2

pair of jet
vortex

deformed velocity
profile
(due to jet/crossflow
interaction)

D

Jet Stream
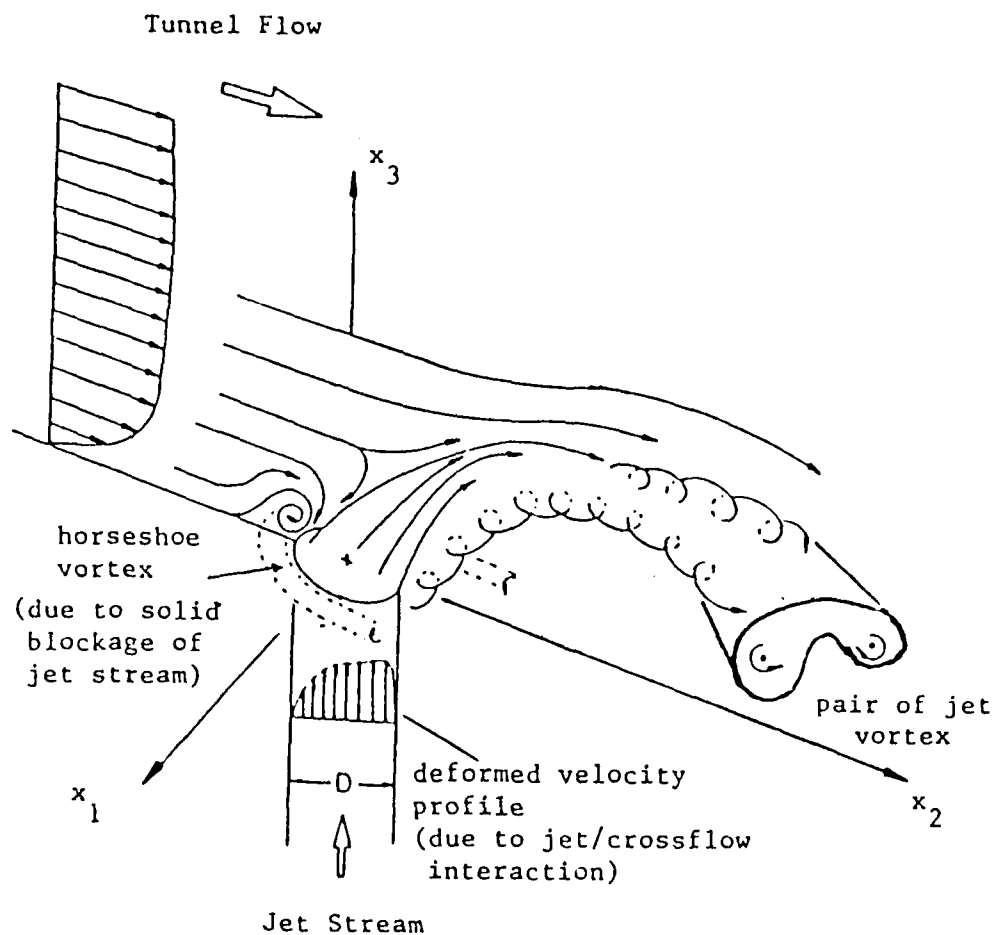
Note: The vorticity contents in jet far upstream
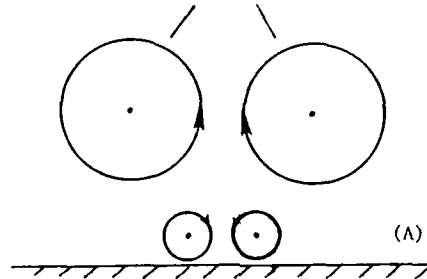is a vortex ring type with components in
x_1 and x_2 direction only.

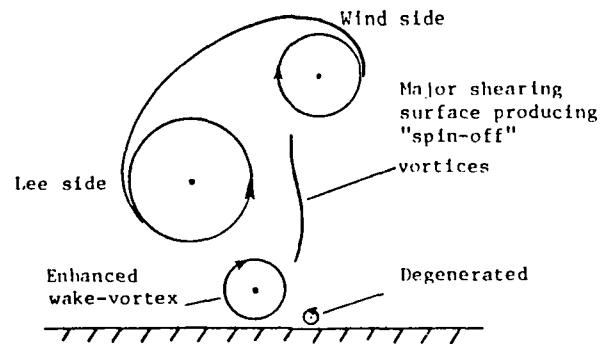Figure 2.2. Sketch of the interaction between a jet an crossflow. (Yu 1987)

11

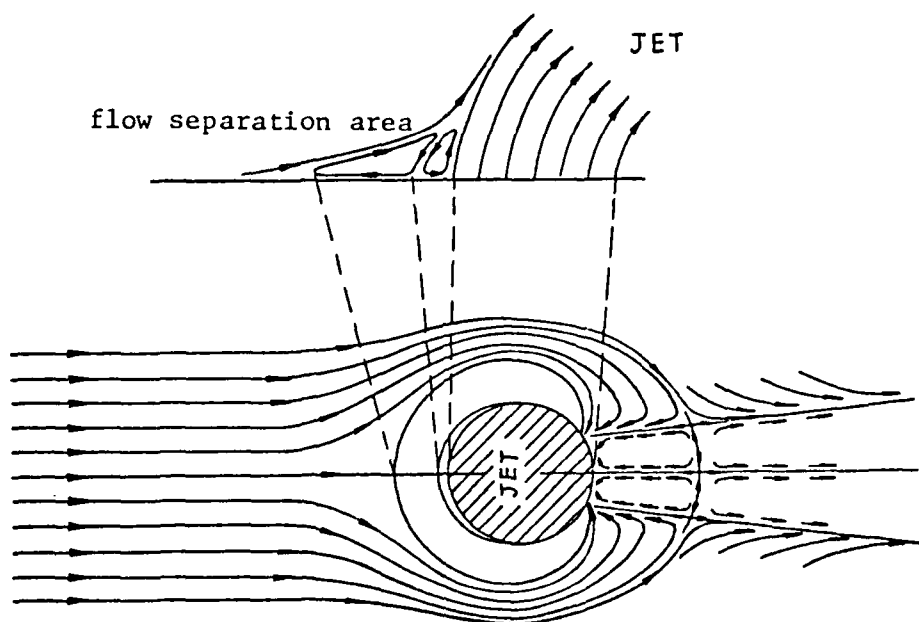Figure 2.3. Non-symmetric jet in crossflow. (Wu, Vakili & Yu 1986)

Counter rotating jet vortices

(a) Vertical sectional view of circular jet in crossflow

Wind side

Major shearing surface producing "spin-off"
vortices

Lee side

Enhanced wake-vortex

Degenerated

(b) Vertical sectional view of asymmetric jet in crossflow

Figure 2.4. A sectional sketch of jet induced vortices in crossflow.
(Wu, Vakili & Yu 1986)

13

JET

flow separation area

JET
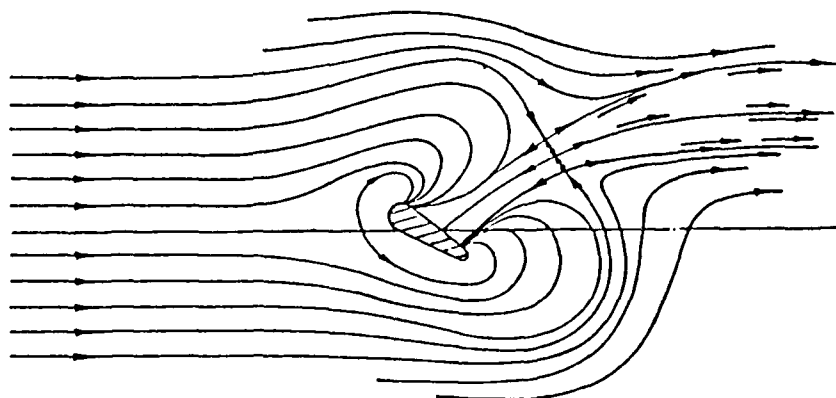
(a) circular jet

(b) Tear drop shaped jet

Figure 2.5. Surface flow pattern around the jets. (Wu, Vakili & Yu 1986)

14

(a) periodic vortices shedding from a circular jet in crossflow, $V_j/V_\infty = 6.3$ (Yu 1987).
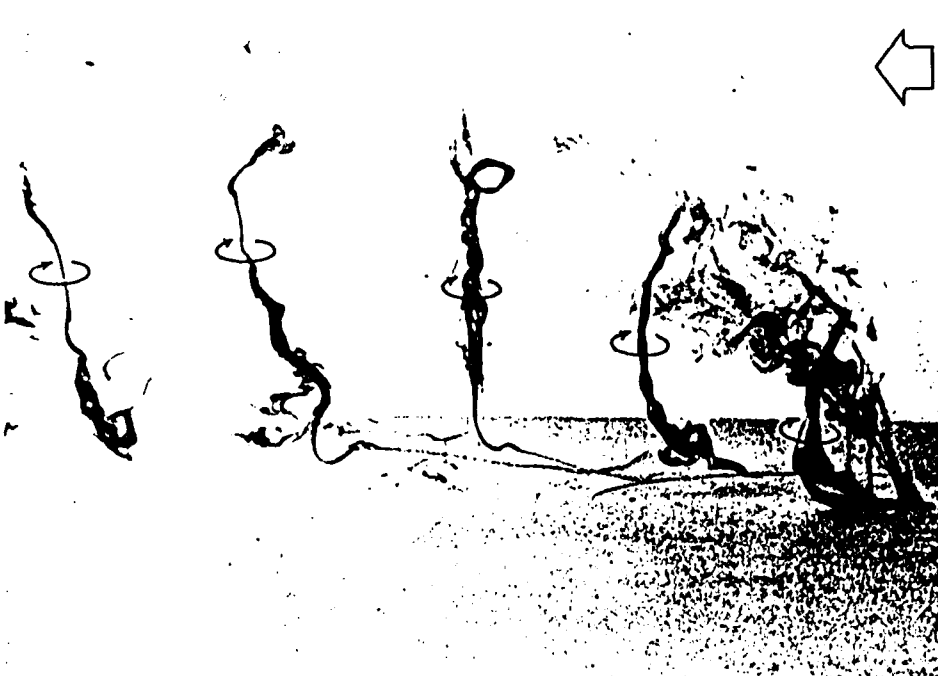
(b) shedding from a non-symmetric jet, $V_j/V_\infty = 3.3$, Red = 240 (Wu, Vakiii & Yu 1986).

Figure 2.6. Periodically shed "spin-off" vortices.
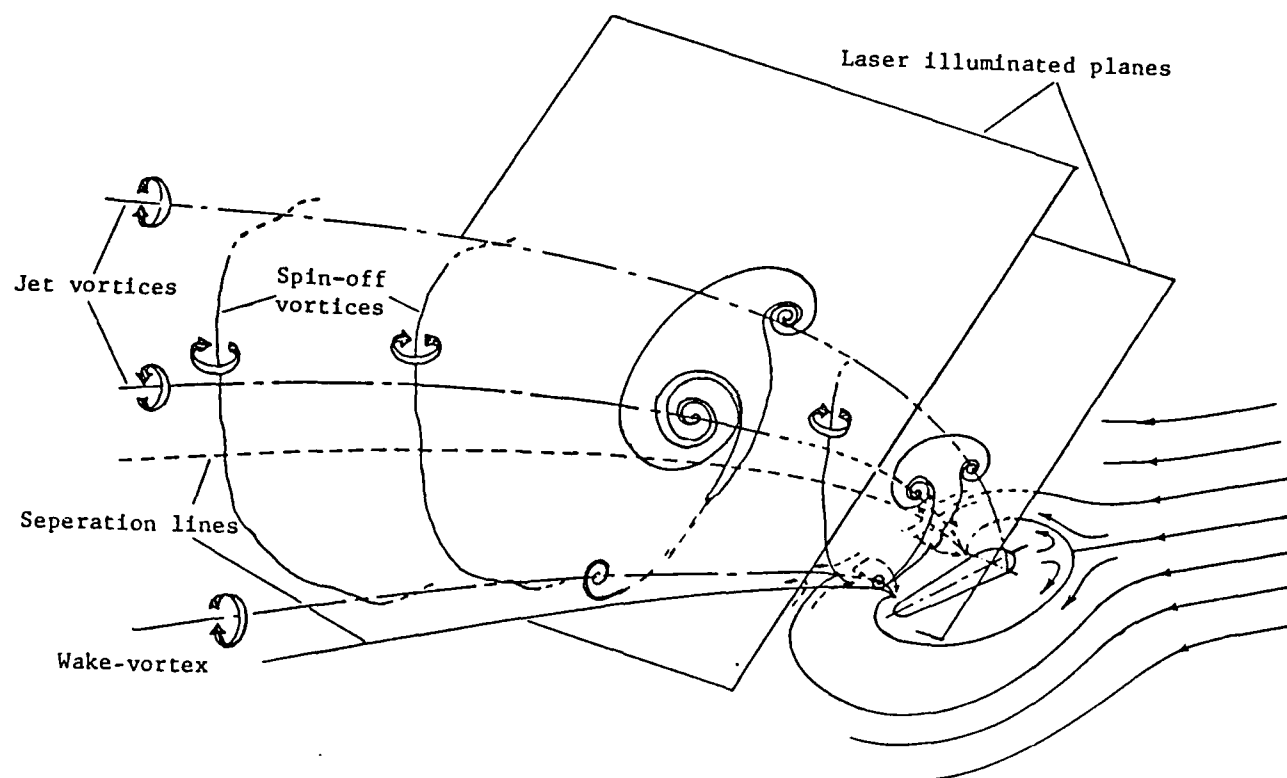
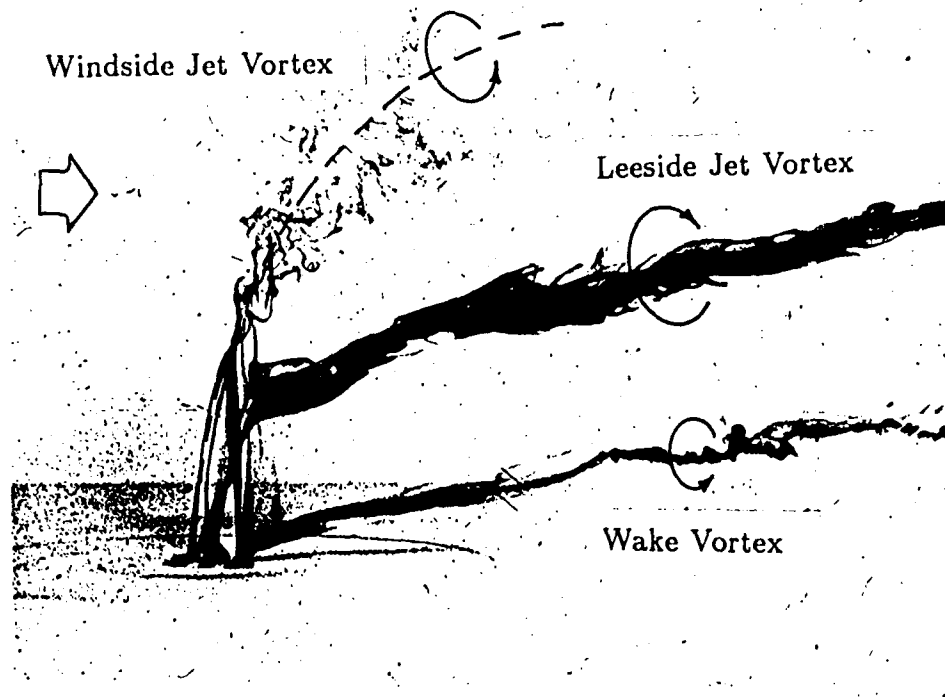Figure 2.7. Schematic of the flowfield of non-symmetric jet in crossflow. (Wu, Vakili & Yu 1986)

16

Figure 2.8. Non-symmetric jet in crossflow, $V_j/V_\infty = 3.7$. Red = 240. (Yu 1987)

of a wingtip jet has the flow of a single jet in crossflow manifested in it.

B. WINGTIP FLOW FIELD

The wingtip wake flow was made visible using dye bleeding from small ports on the wingtip. In Figure 2.9(a), the wingtip vortex core flow persisted far downstream with little dispassion (a well known phenomenon). With the wingtip jets blowing, the tip vortex core was dispersed significantly as shown in Figure 2.9(b). Figure 2.10 shows that wingtip blowing has a similar effect on a rounded shaped wing tip flow. Depending on the combination of location and amount of jets blowing, various degrees of dispassion were reached. In our water tunnel study, larger blowing coefficients compared to the wind tunnel study were used for better visualization and enhancement of the interactions observed. The non-dimensional parameter used in the water tunnel study was the jet momentum coefficient C_μ, defined as

$$C_\mu = \dot{m}V_j/0.5\rho V_\infty^2 S$$

where $\dot{m}$ is jet massflow rate, V_j is jet exit velocity and S is the wing area.

In order to study the details of the jet flow structure, a single jet blowing at different locations were carefully investigated. The flow pattern of a single jet on wingtip was similar to those for a plane jet which has been described in section 2.3.(a) with the exception of the wingtip effect. Figure 2.11(a) is a photo of a typical single wingtip jet flowfield, and a sketch of this flowfield is shown in Figure 2.11(b). The flow pattern is very similar to that shown in Figure 2.3.

On the near field close to the jet, a typical non-symmetric jet in crossflow interaction started to form, the original wingtip effect was only through changes in the on-coming flow direction. Near the wing surface, the fluid moved around the jet and only leaves the surface from the wake side of the jet flow as shown in Figure 2.12, which is the similar to those shown in Figure 2.4.

There were two shear layers on each side of the jet flow, it was sustained by the pressure gradient across the jet. Due to the wake unsteadiness, these shear layers broke
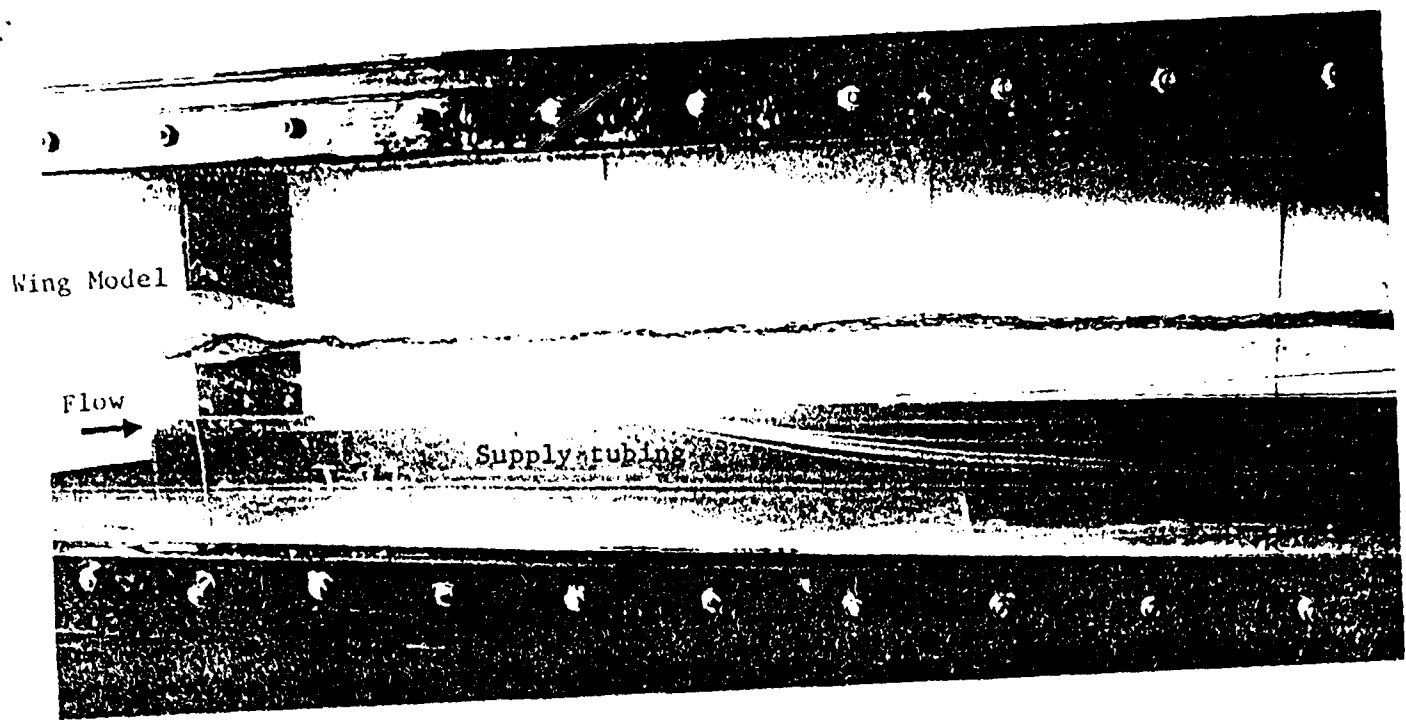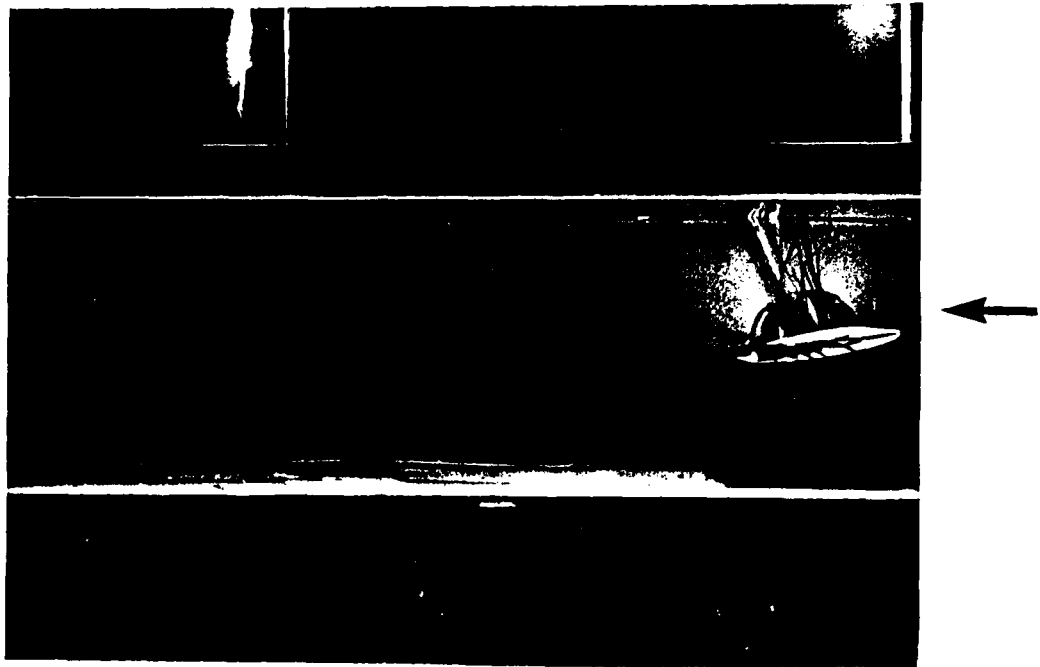
(a) without jet blowing
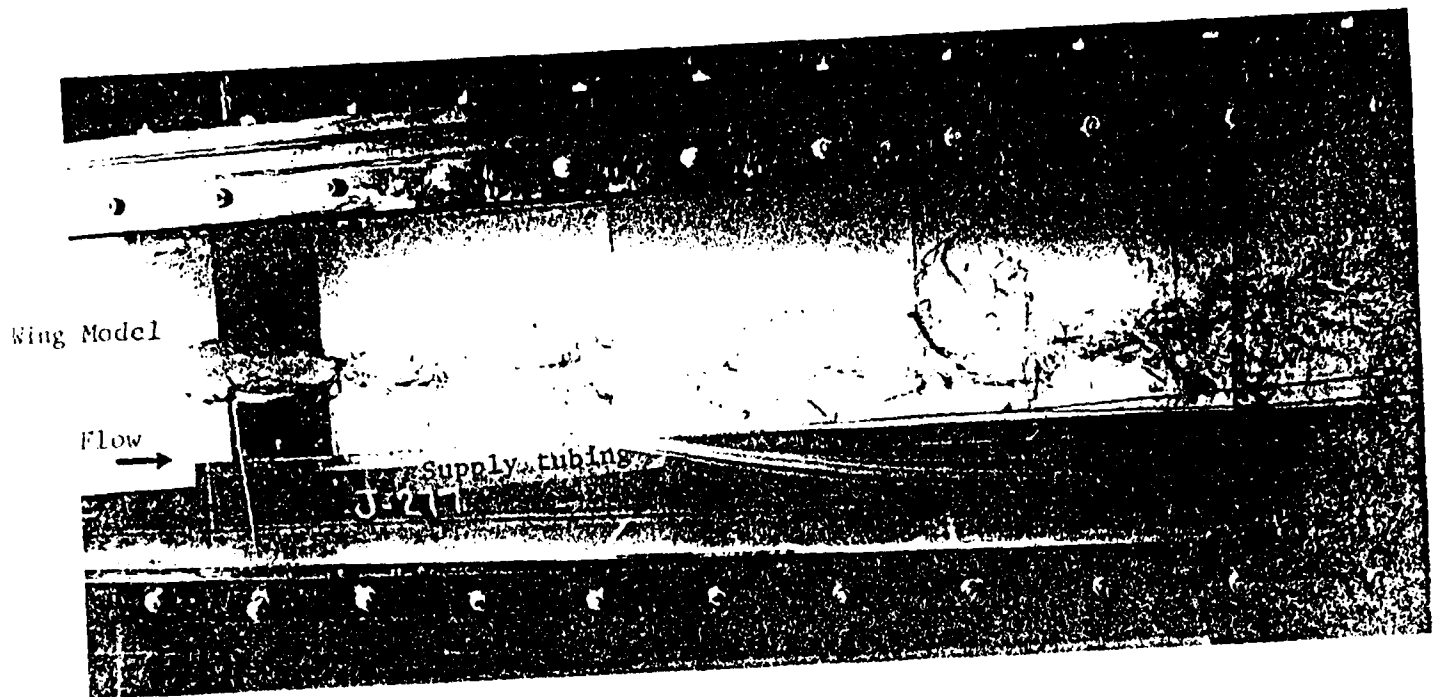
(b) with jet blowing from front jet

Figure 2.9. The effect of wingtip jet blowing on tip vortex for a rectangular wingtip. (Wu & Vakili 1984)
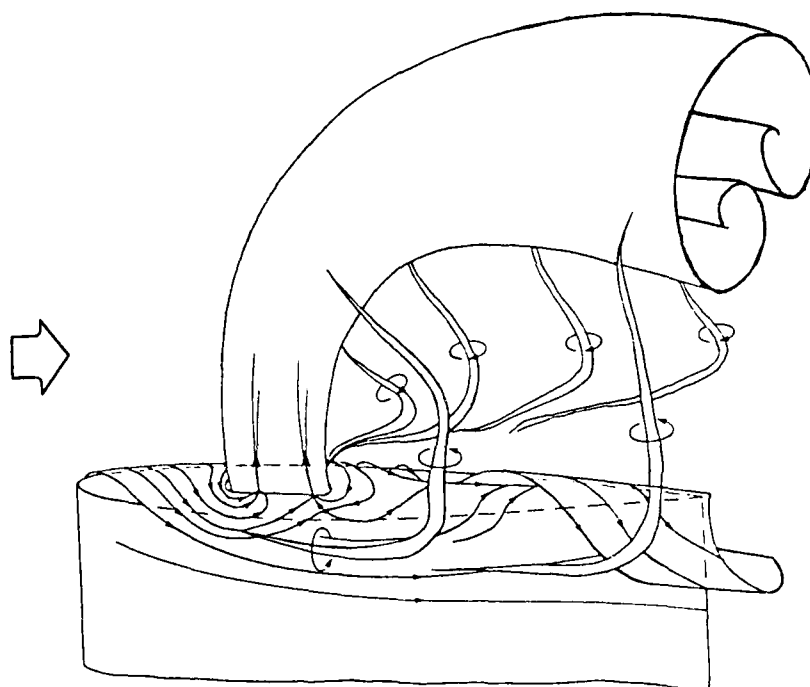
19

(a) without jets

(b) with jets blowing

Figure 2.10. The effect of wingtip jet blowing on tip vortex for a rounded wingtip.
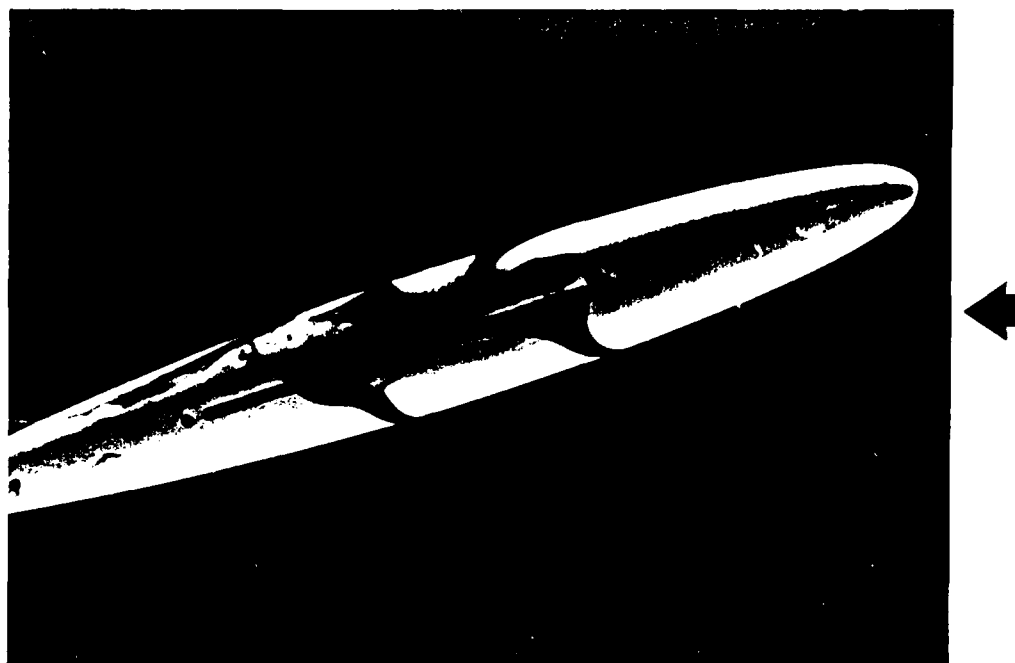
20

(a) front jet blowing ($V_\infty = 4.3$ cm/s, $\alpha = 24^o, C_\mu = 0.07$)

(b) a sketch of single jet flowfield

Figure 2.11. Single wingtip jet flow flowfield.

(a) near surface flow at jet #1
     ($V_\infty = 8$ cm/s, $\alpha = 16°, C_\mu = 0.02$)

(b) top view

Figure 2.12. Near furface flow pattern for single jet.

22

down to form "spin-off" vortices under certain conditions. The top of the jet flow has a kidney shape cross section and the flow were fully turbulent as shown in Figure 2.11.

Some distance (2 to 3 cm) upstream of the jet, the flow pattern appeared the same as those without jet blowing, that is, the flow moved from the lower to the upper surface of the wing. However, due to the presence of the wingtip jet flow, the flow did not roll-up to form a tip vortex as it would in a no-blowing case. This flow pattern is shown in Figure 2.13.

About 1 to 2 cm downstream from the jet, the flow pattern near the wing surface gradually returned to the usual wingtip flow pattern. It rolled-up from the bottom to the top surface but with lesser rotational tendency than that in a no-blowing case. This phenomenon is also shown in Figure 2.13.

The wake of the wingtip with tip jet blowing had much less roll-up tendency than it had in the original no-blowing case. It moved downstream with very little global rotation and contained many vortices. The wake of the wingtip jet crossflow was very unsteady. With the wingtip jet blowing, the cross-section of the tip wake flow enlarged considerably than without blowing, a comparison of the two cases, Figures 2.9 and 2.10 clearly shows this fact. The wake moved upward and outward from the wing tip due to jet blowing and its vortex roll-up structure became much looser than that in a no-blowing case where the tip vortex rolled-up tightly.

If a jet was placed too close to the leading-edge, the wake would partly roll-up after some distance downstream; on the other hand, if the jet was placed too close to the trailing-edge, the roll-up would form before the jet. From the above observations, we realized that there was a critical position of the jet port which may lead to a favorable effect on dispersion of wingtip vortex. Our wind tunnel test results verified this conclusion.

Two or more jets blowing simultaneously increased the dispersion effect, however, this operation is usually associated with more mass flow rate. If two jet ports are placed far apart and with a smaller C_μ, then each individual jet would behave the same as a single jet. There would be an interaction between two jets if they are closely placed and with higher C_μ. Flow pattern for two jets blowing is shown in Figure 2.14, owing to the small
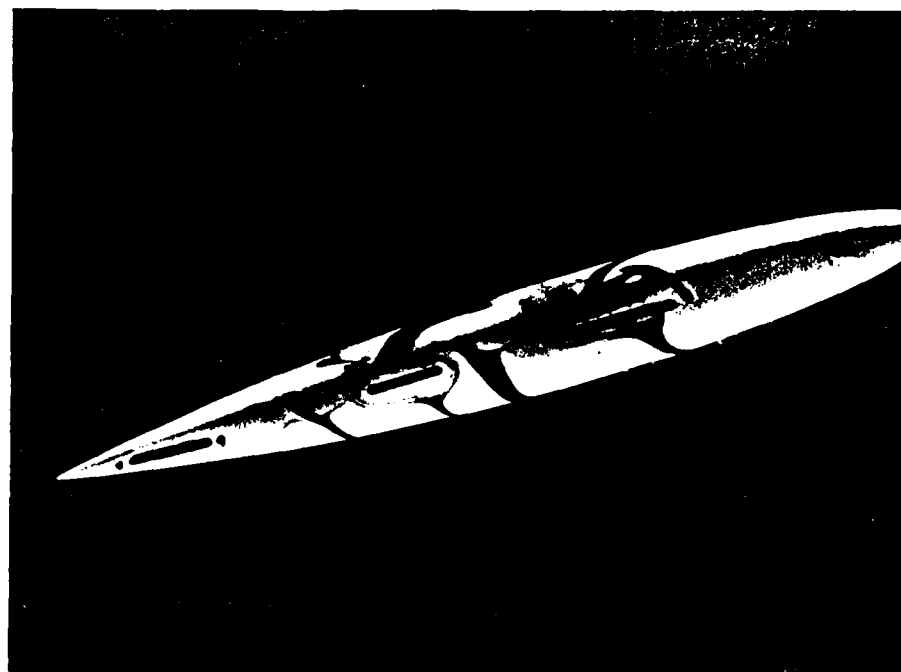
23

(a) side view

(b) top view

Figure 2.13. Global view of the flowfield for a single jet blowing. (jet #2, $V_\infty = 8$ cm/s, $\alpha = 16^o, C_\mu = 0.02$)
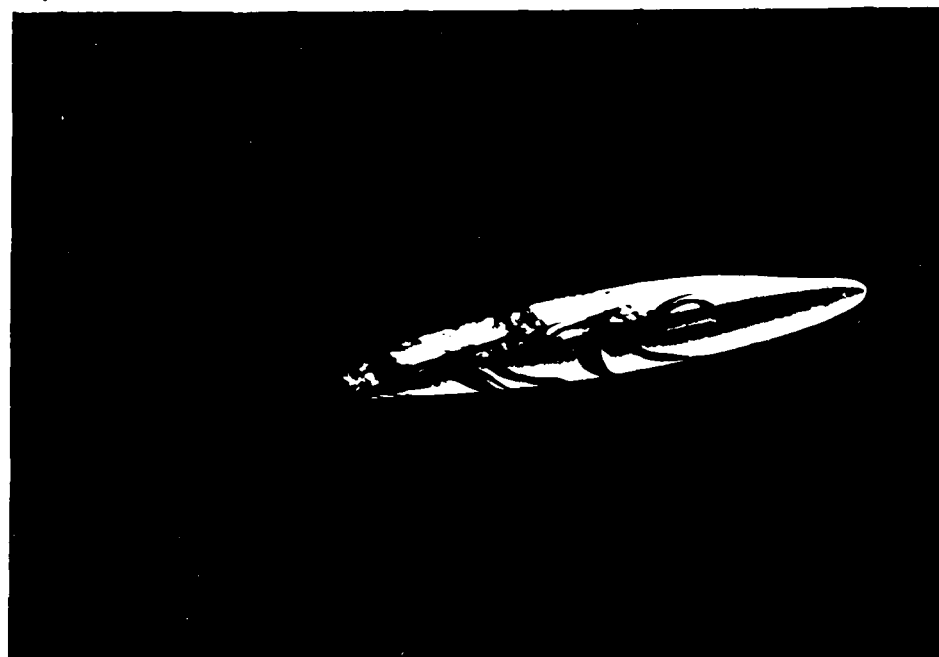
24

(a) side view

(b) top view

Figure 2.14. Near surface flow pattern of two jets blowing. ($V_\infty = 8$ cm/s, $\alpha = 16^\circ$, $C_{\mu I} = C_{\mu II} = 0.02$)

C_μ for each of the jets the mutual interaction is small. Figure 2.15 shows a photo of three jets blowing.

In general, more jets blowing with higher C_μ will lead to a better dispersion of the wingtip vortex.

(a) side view

(b) top view

Figure 2.15. The flow pattern of three jets blowing. ($V_\infty = 8$ cm/s, $\alpha = 10°$, $C_{\mu I} = C_{\mu II} = C_{\mu III} = 0.01$)

27

III. WIND TUNNEL EXPERIMENTS AND RESULTS

The studies conducted in the wind tunnel were surface oil flow, surface pressure distribution and the wake surveys. The wake survey study has not been completed yet and is still in progress.

3.1 WIND TUNNEL FACILITY AND MODEL

All the wind tunnel experiments were conducted at The University of Tennessee Space Institute (UTSI) low speed wind tunnel. This facility has an open circuit continuous wind tunnel with a closed test section. The test section was 35.6 cm height, 50.1 cm width and 107 cm length (H 14 in. x W 20 in. x L 42 in.), it has a Plexiglas side wall for observation and photography. The tunnel was driven by a 1.14 m diameter fan which was powered by a 75 HP motor and has a velocity range from 3 to 90 m/sec (10 to 300 ft/sec). Tunnel operation control and data acquisition was digital and handled by small computers.

The model used for wind tunnel tests was a NACA 0012-64 airfoil with 18.0 cm chord length and 30.48 cm half span. The model was made such that there was access from within to the wingtip, for the purpose of wingtip jets and pressure ports. The wing tip had three tip jet ports on it and the blowing air was supplied to the individual tip jets through separated tubes. A sketch of the wing model is given in Figure 3.1. Pressure ports were provided at four span sections. There were 12 pressure ports on the upper surface and 12 on the lower surface for each row as shown in Figure 3.1.

The model was supported by a shaft through the tunnel side wall to a machinist turntable which had the capacity of continuous incident angles setting of 0° to 360°. A boundary layer fence was installed between the model and tunnel inner wall to ensure local two dimensional flow. Figure 3.2 shows the wind tunnel experimental set up.

The blowing air was supplied by a 150 psia (Pennsylvania) low pressure compressor. A pressure regulator controlled the air pressure entering to a flowmeter downstream of it.
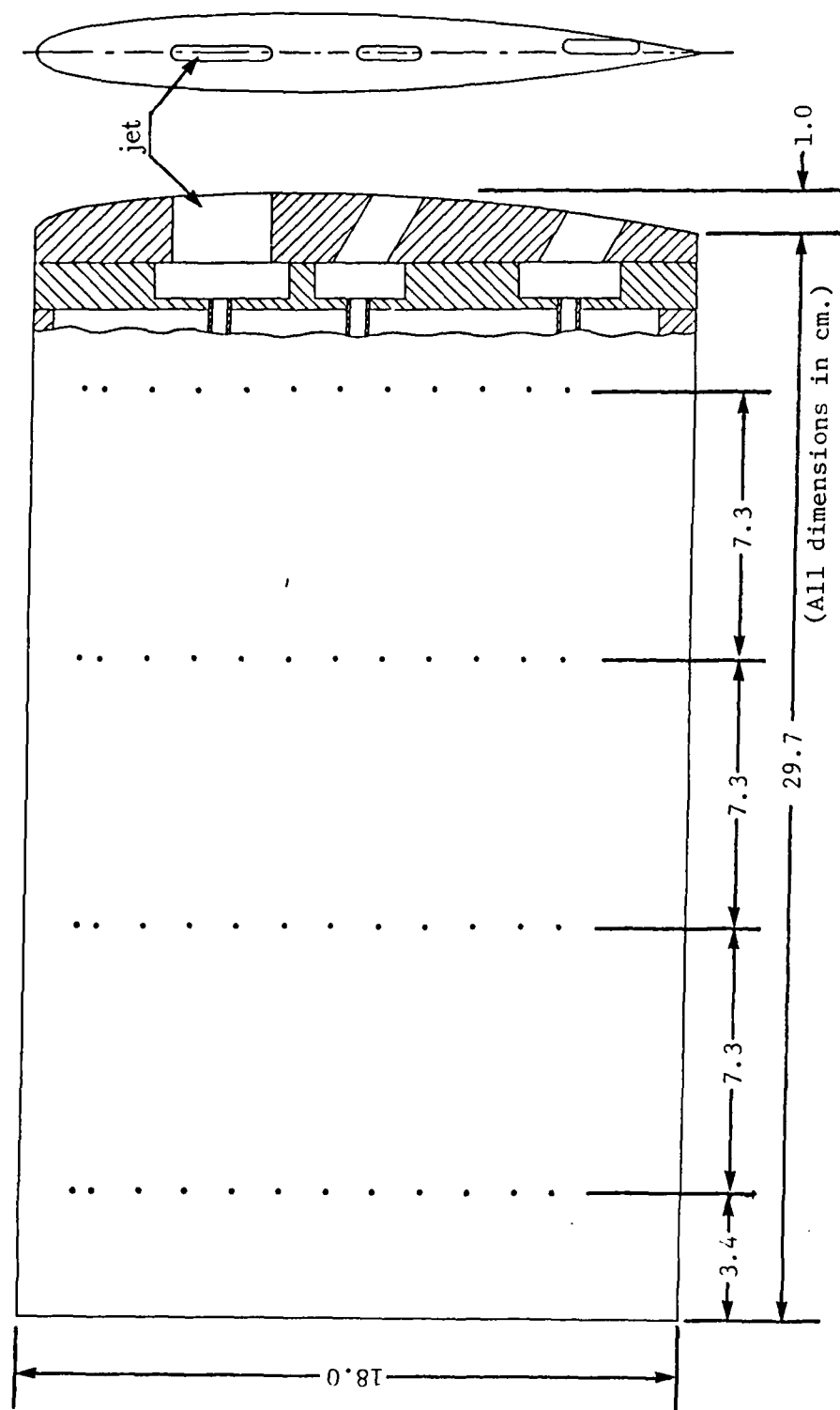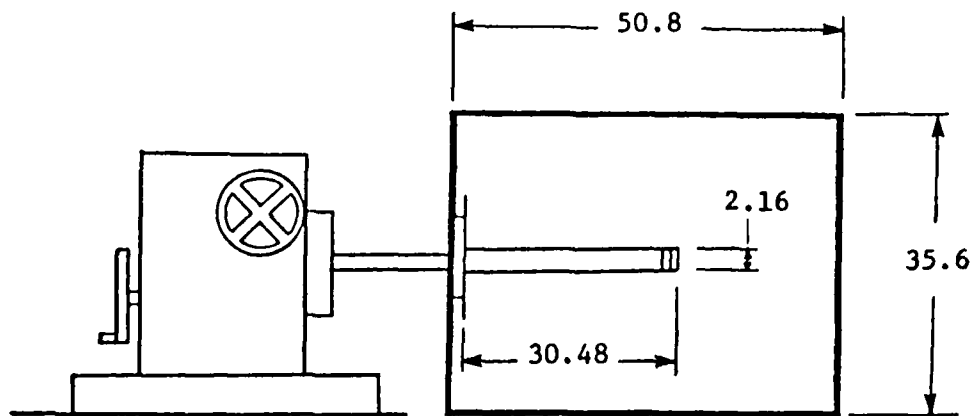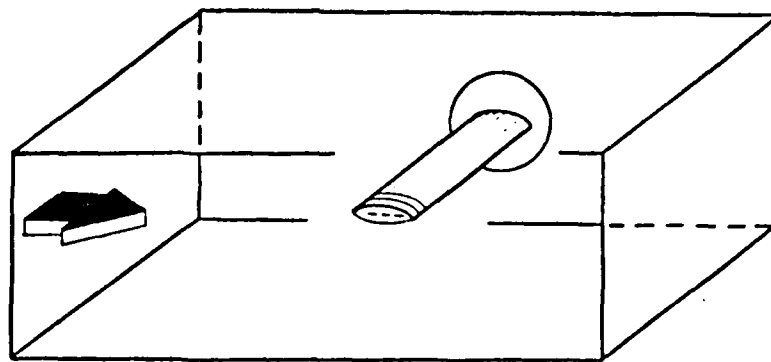
28

Fifure 3.1. Schematic of the wind tunnel wing model.

Dimensions in centimeters

(a) schematic of sting mounted half-wing model

(b) pictorial view of test section

Figure 3.2. Experimental set-up in the wind tunnel.

30

The volume ratio of the blowing air was controlled by a valve installed downstream of the flowmeter. From the pressure reading at the regulator and the air volume at the flowmeter, the air flow rate $\dot{m}$ was calculated. The non-dimensional parameter used in wind tunnel study was also the jet momentum coefficient C_μ, which was defined as

$$C_\mu = \dot{m}V_j/0.5\rho V_\infty^2 S$$

where V_j is the jet exit velocity, V_∞ is the tunnel velocity and S is the wing area. Restricted by the jet areas and pressure restriction of the flowmeter, the $C\mu$ values used in this wind tunnel experiment were relatively smaller than what was used in the water tunnel study.
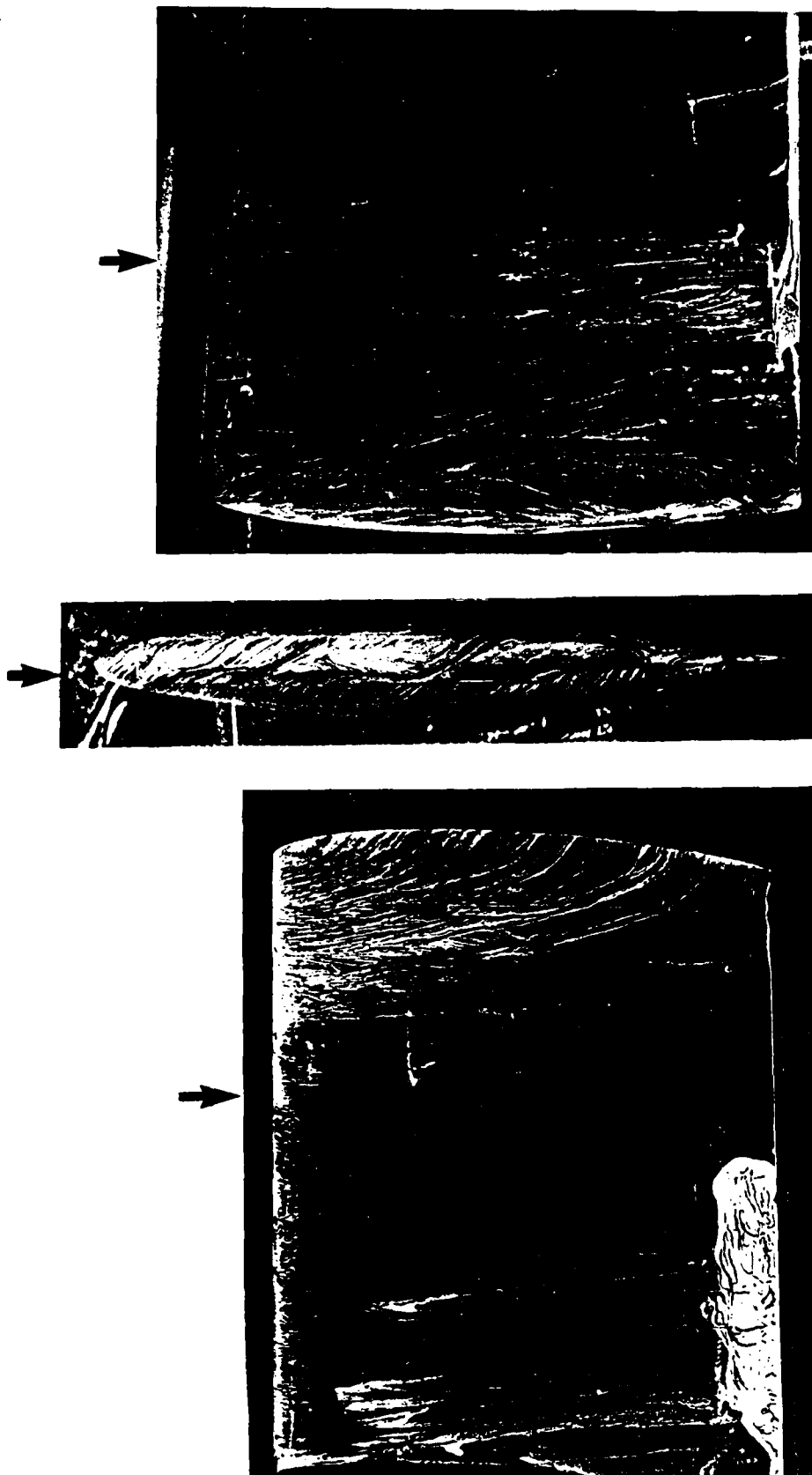
3.2. SURFACE OIL FLOW

Surface oil flow visualization was used to obtain qualitative results similar to the water tunnel and to improve the physical understanding of the complicated three-dimensional flow around the wing in the wind tunnel testings. Although this method displays only the footprints of the flowfield on the surface of the model, together with water tunnel observation it gives detailed qualitative information on the flow structure and pattern.

The oil used was a mixture of kerosene and white oil paint in such a way that it moved with the flow when the tunnel was started and it normally dried on the wing surface after 1 to 2 minutes. The tunnel speed reached its set value in about 10 seconds and thus the oil trace represented the steady state flow.

Figure 3.3 is a typical surface oil flow pattern on the wing model without tip jet blowing, at $V_\infty = 45$ m/sec and angle of attack $\alpha = 10°$. At moderate angles of attack, there was a small separation region on the upper surface.

Near the wingtip, the low pressure on the upper surface caused the flow to move faster and no separation was observed. On the wing tip, a narrow separation strip was observed. This was because of the tip flow rolled-up from the bottom to top in such a way that the flow could not be sustained on the surface all the way. For the rectangular wing tip case,

31

(a) low surface

(b) tip

(c) upper surface

Figure 3.3. Surface oil flow pattern for no-blowing case, $V_\infty = 45$ m/s, $\alpha = 10°$.

32

the separation area was much larger and almost covered the whole wingtip. The wind tunnel oil surface flow results were consistent with water tunnel observations.
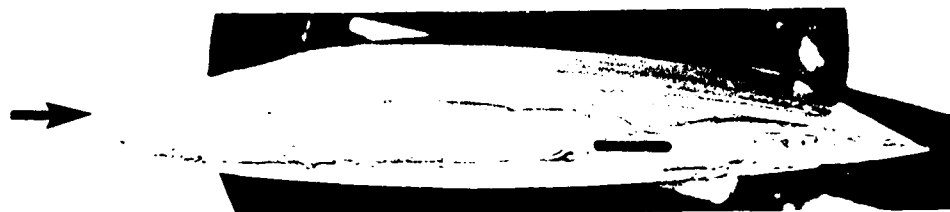
A surface oil flow pattern for the wing with wingtip jet blowing is shown in Figure 3.4. Compared to the surface flow pattern for no-blowing case (Figure 3.3), the surface flow structure changed at several places. Changes were observed at the neighborhood of the wingtip. The flow pattern near the jet exit was very much like that shown in Figure 2.5(b), and was consistent with the near surface flow pattern results observed in the water tunnel study. In addition, the dividing line on the upper surface of the wing moved toward the wingtip. This indicated that the intensity of the wingtip vortex cone was reduced. Other changes observed were the separation bobble at the trailing-edge of lower surface moved toward the root of the wing and reduced in size. It was also observed that the separation zone along the trailing edge of the upper surface changed by blowing. It became larger than that in no-blowing case, this implied that the aerodynamic loading of the wing model increased in latter case.

## 3.3. SURFACE PRESSURE MEASUREMENT AND LIFT COEFFICIENT

The motivation for doing surface pressure measurement was to observe how the wingtip jet blowing affected the pressure distribution on the whole wing surface. The results showed that the wingtip jet blowing led to a global improvement, i.e., the sectional C_l distribution was improved over the entire chord as well as in spanwise.

The surface pressure were measured by four ±1.3 psid. transducers which were used with two 24 ports wafer switches. The pressure transducer signal was put through a Validyne Amplifier, a Lab Master A/D converter and collected to an IBM PC/XT compatible computer. The data were first checked on the PC computer, and then sent to the UTSI VAX 11/785 computer through a communication line for further analysis and plotting.
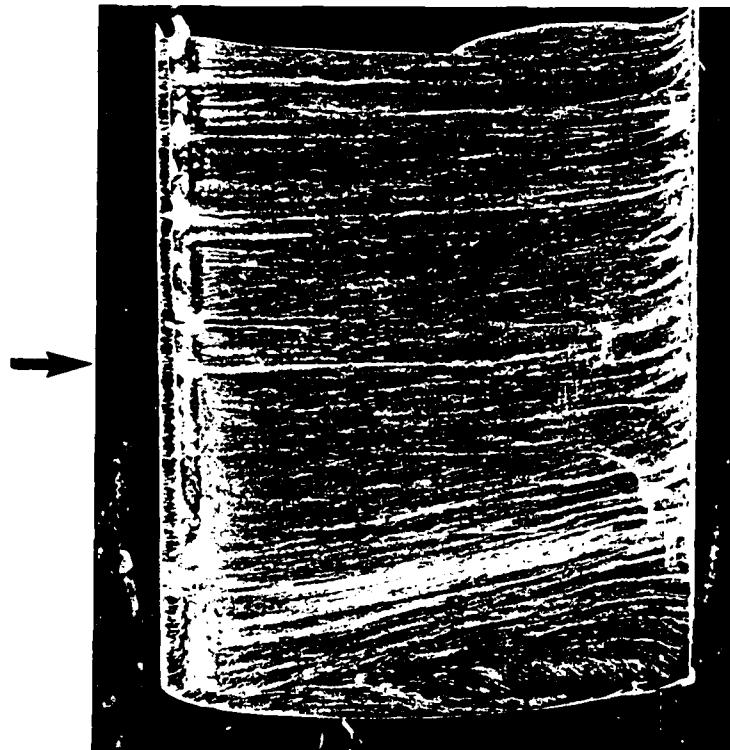
Some typical comparisons of the pressure distribution on the wing surface with and without jet blowing are shown in Figure 3.5 and 3.6. It is clearly shown by these figures
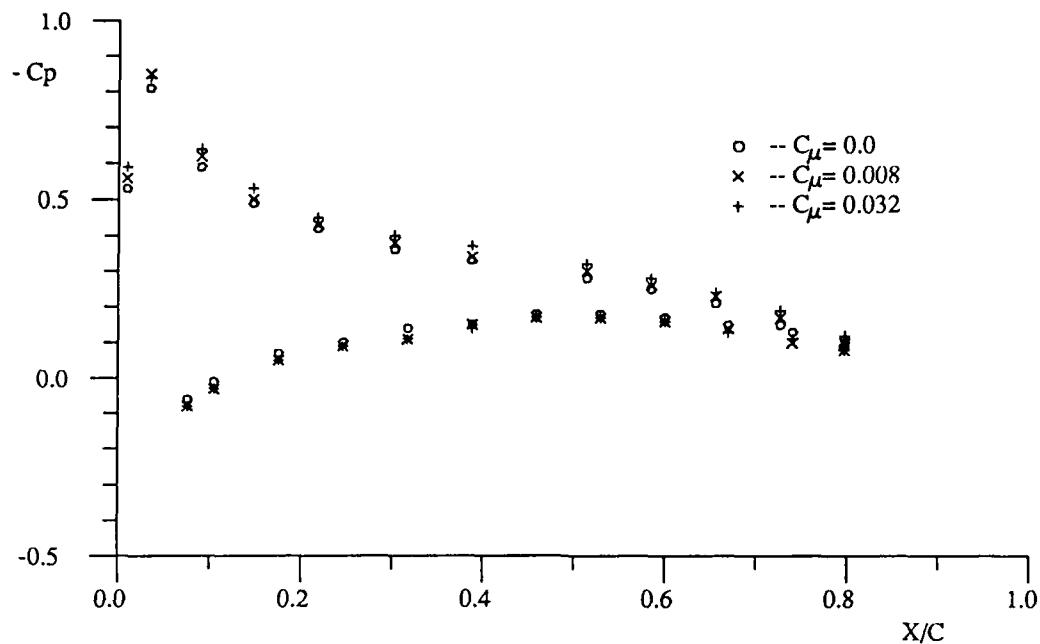
(c) upper surface

(b) tip
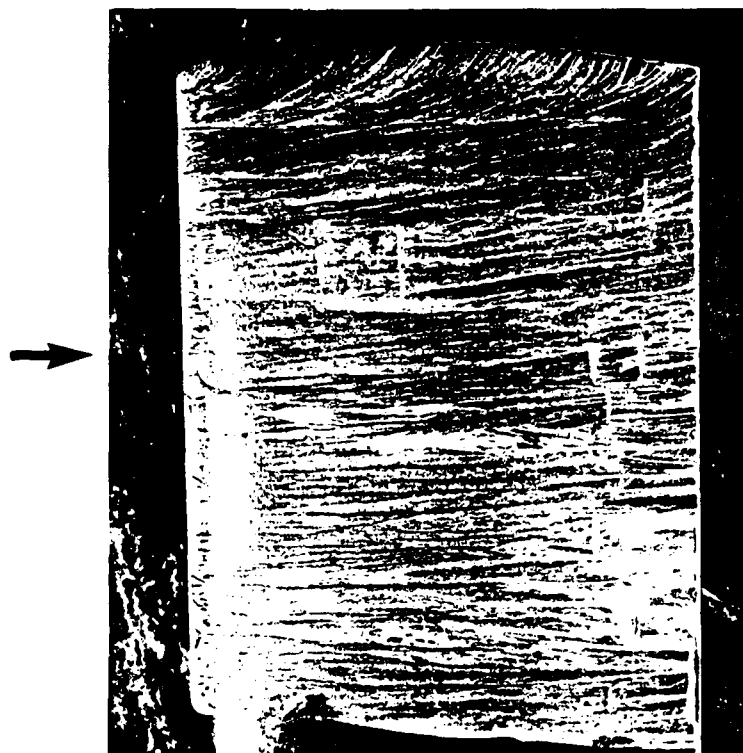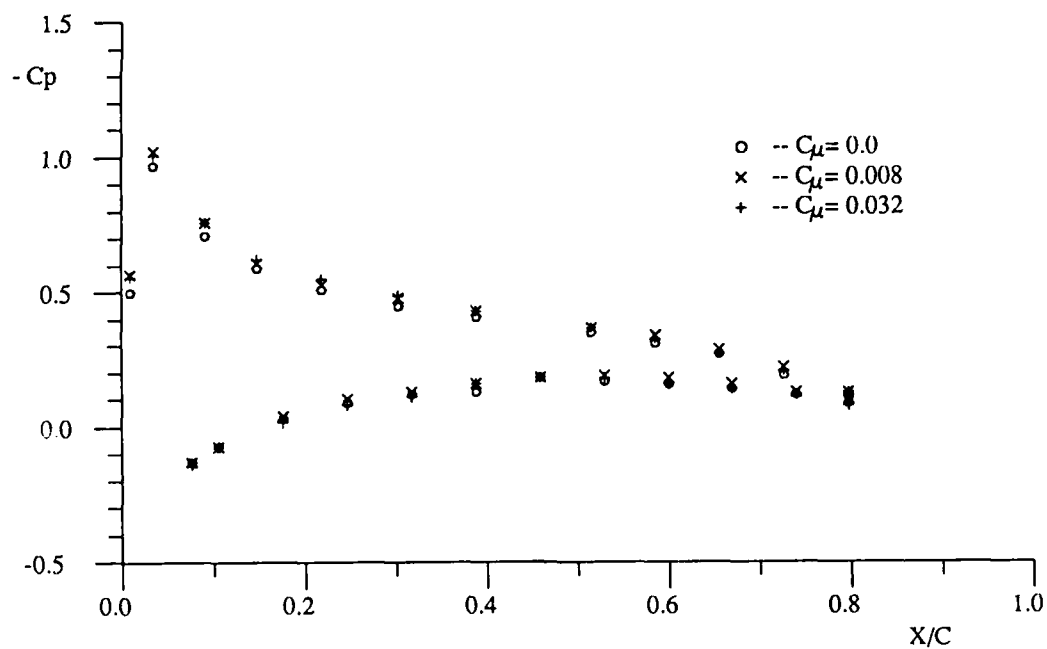
(a) low surface

Figure 3.4. Surface flow pattern for the wing with 2nd jet blowing, $V_\infty = 45$ m/s, $\alpha = 10°$, $C_\mu = 0.002$.

34

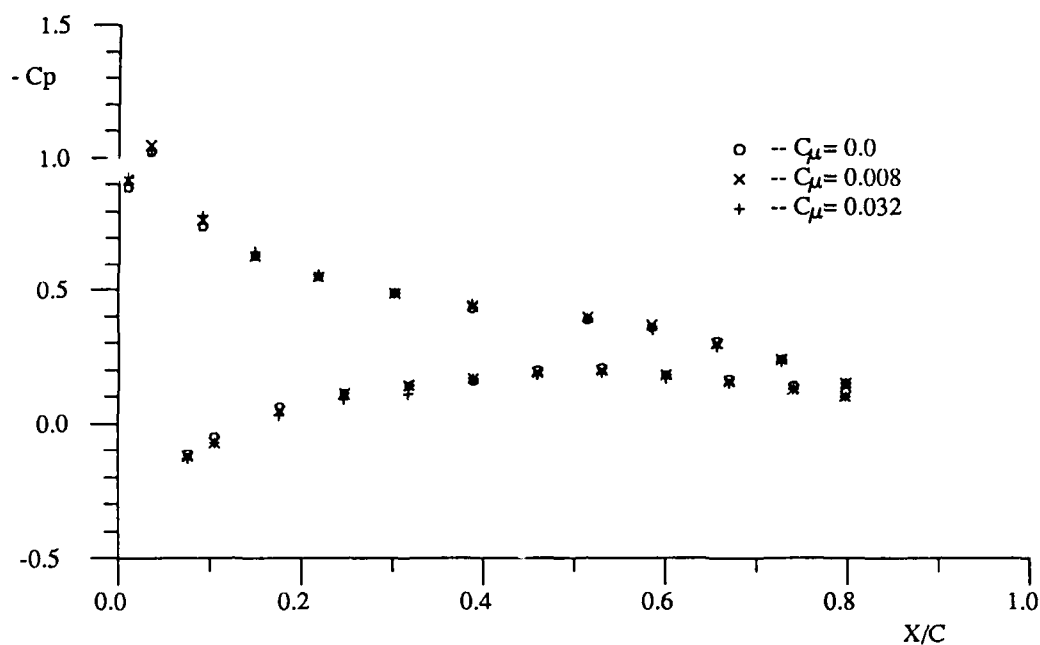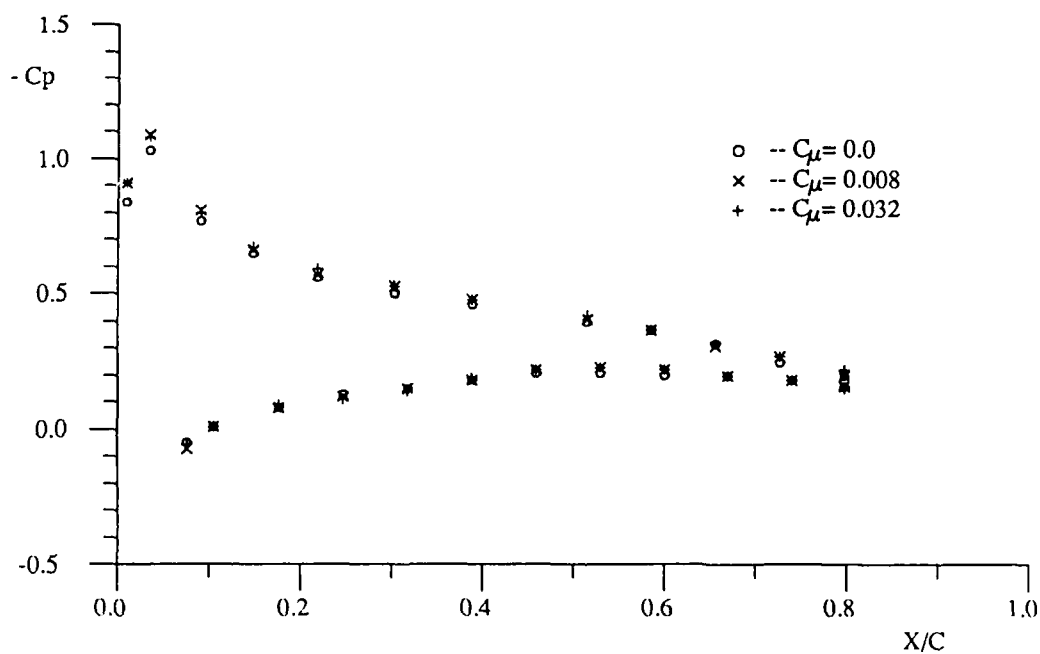(a) . Cp distribution at 2Y/B = 0.826.

(b) . Cp distribution at 2Y/B = 0.588.

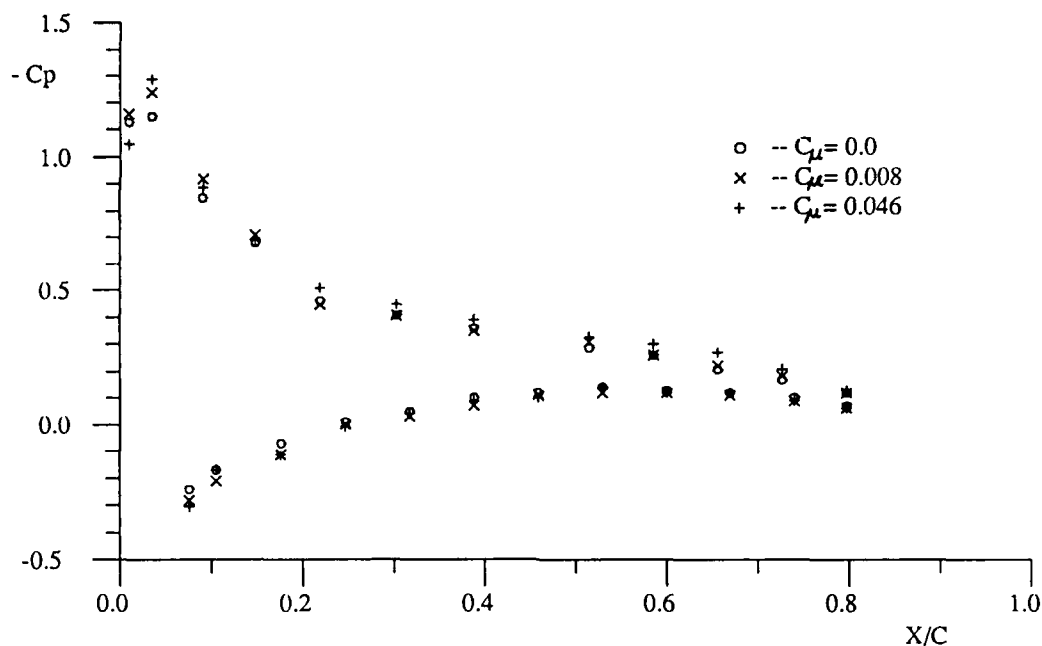Figure 3.5. Chordwise C_p distribution at different section, V_∞= 20 m/s, α=5°, jet 1.
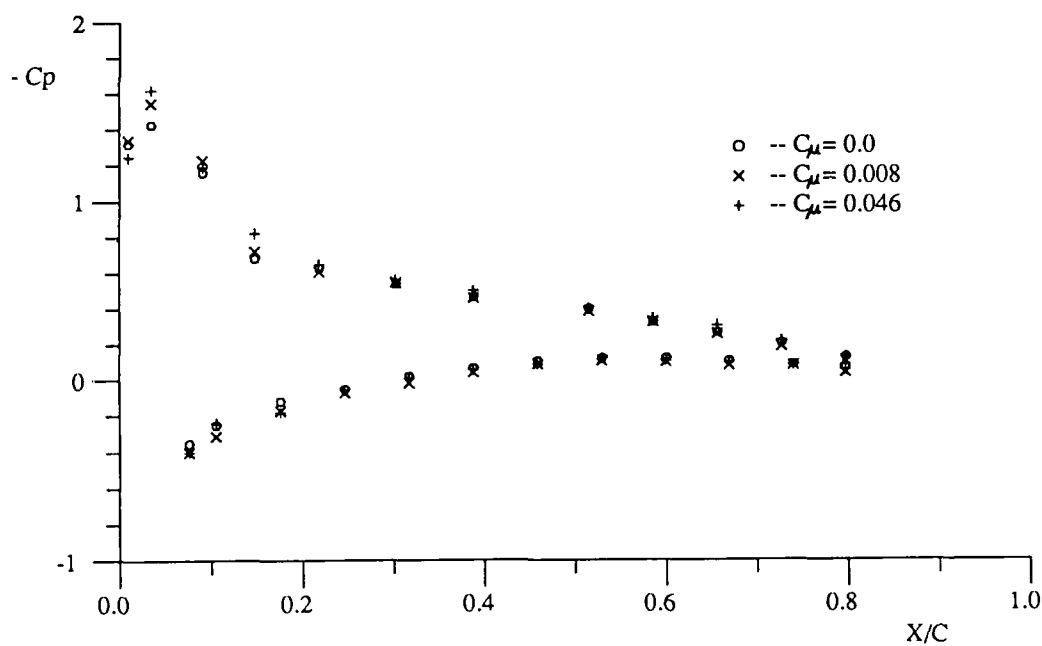
35

(c) . Cp distribution at 2Y/B = 0.350.

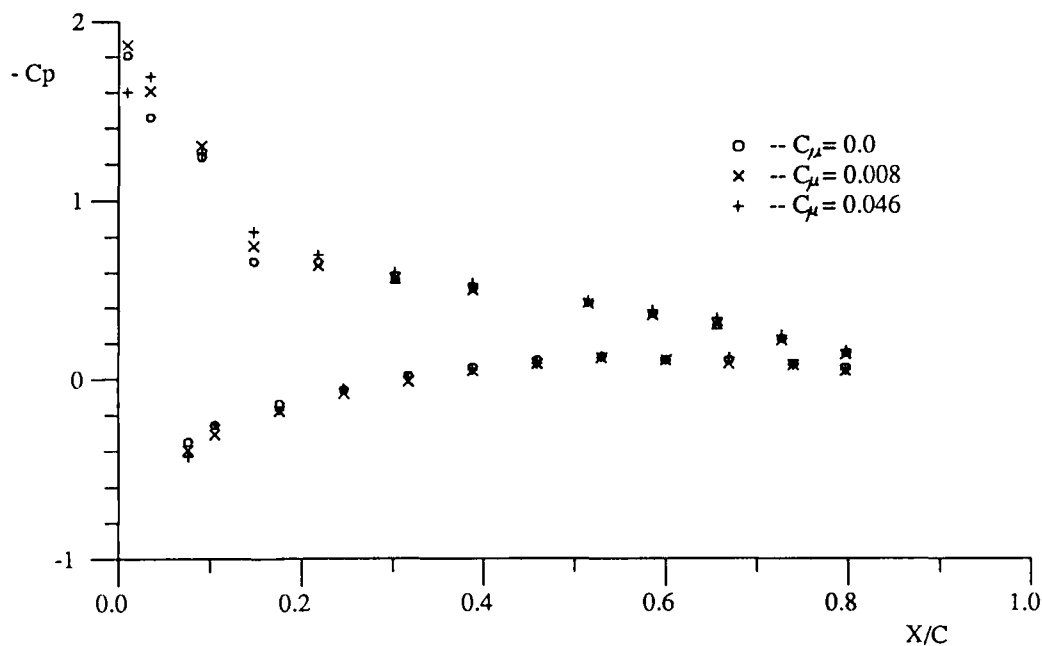(d) . Cp distribution at 2Y/B = 0.1115.

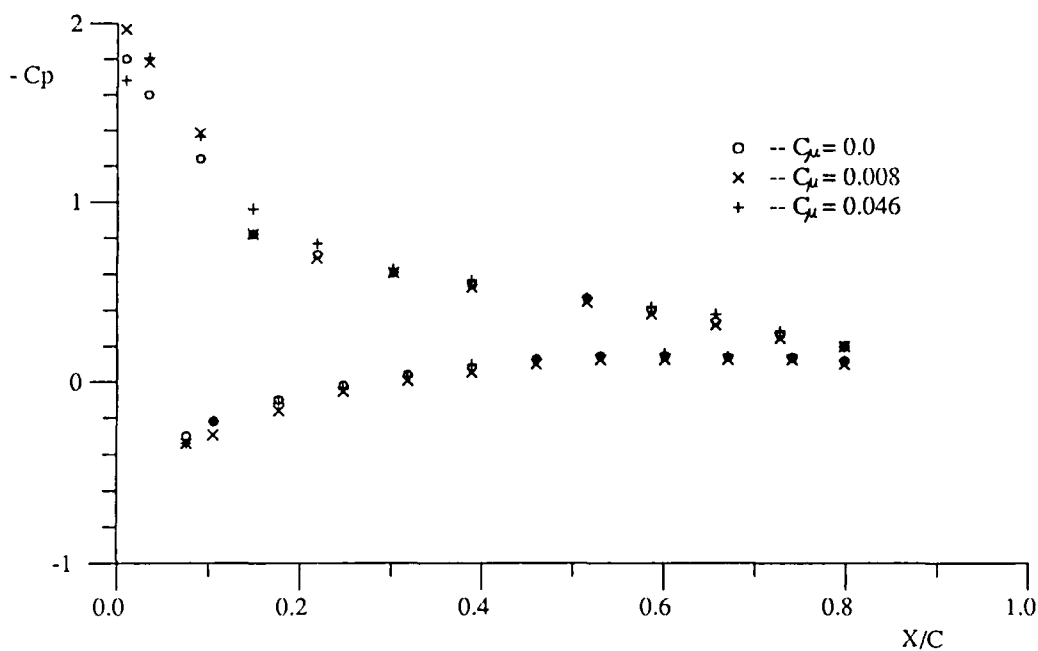Figure 3.5. (continued)

(a) . Cp distribution at 2Y/B = 0.826.

(b) . Cp distribution at 2Y/B = 0.588.

Figure 3.6. Chordwise C_p distribution at different section, $V_\infty = 20$ m/s, $\alpha=8^\circ$, jet 2.

37

(c). Cp distribution at 2Y/B = 0.350.

(d). Cp distribution at 2Y/B = 0.1115.

Figure 3.6. (continued)

that the lift coefficient (C_l distribution) was improved by the wingtip jet blowing. And in general, a larger blowing coefficient C_μ results in a larger ΔC_l. The results show that the improvement in the pressure distribution was different from that of the winglet. The winglet utilizes the principle of pressure superposition and its effect were mainly localized. In the wingtip jet case, the pressure improvement was observed over the entire chord and span, i.e., a more global improvement over the wing was obtained. This implied that the original wing circulation and the vortex system were changed by the jet blowing which qualitatively agrees with observations from the water tunnel and surface oil flow tests of the wind tunnel.

Spanwise lift distributions were estimated by the chordwise integration of surface pressure measurements. Since there were 12 pressure ports along chordwise direction, the chordwise line integration was used. While along the span there were only 4 section points, so curve fitting and numerical integration were used.

Figure 3.7 and 3.8 show two spanwise C_l distributions which correspond to the data in Figure 3.5 and 3.6. It is observed in these figures that the pressure coefficient changed favorably over the whole wing span by the wingtip jet blowing.

It was found that although the pressure distribution improved on the whole wing surface, the increments reduced slightly from the wingtip to the root of the wing, the greatest lift increments were near the wing tip (see Figure 3.7 & 3.8). This was because the changing of the flowfield by the wingtip jet blowing was larger near the tip region than that near the root of the wing.

Typical experimental results of C_l vs. C_μ are given in Figure 3.9. The C_l behaved as a linear function of C_μ. This result was consistent with those observed in Reference [14], which is shown in the same Figure.

The experimental results showed that the blowing from the third jet alone was least effective. This was consistent with the water tunnel observations; since the tip vortex already rolled-up before reaching the jet port 3 location and made the jet-3 less effective, which was also consistent with the result given in Reference [14].
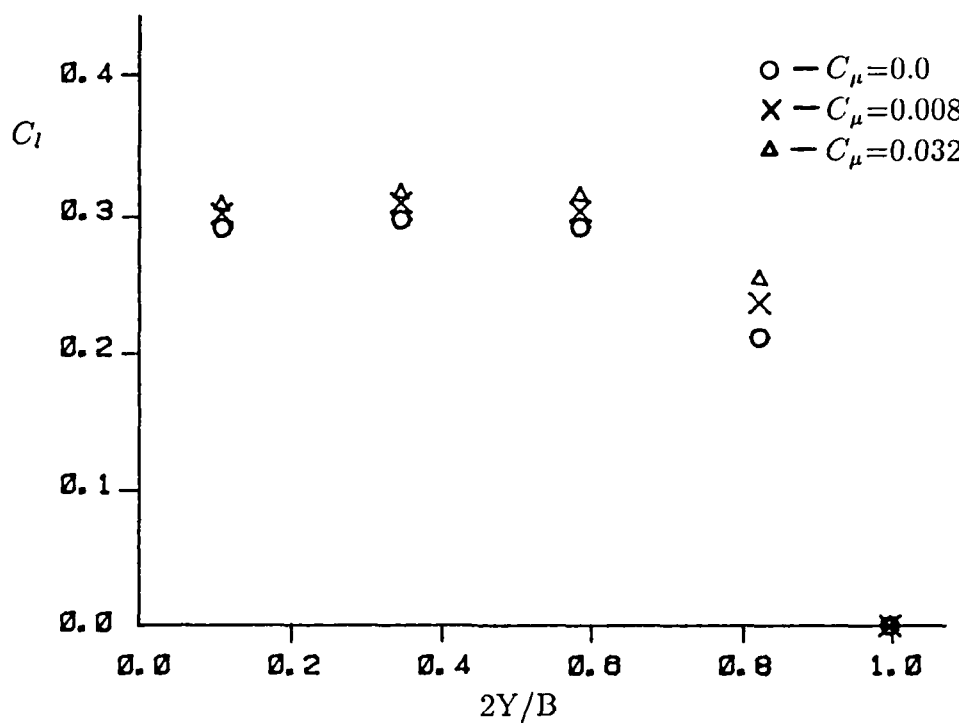
39

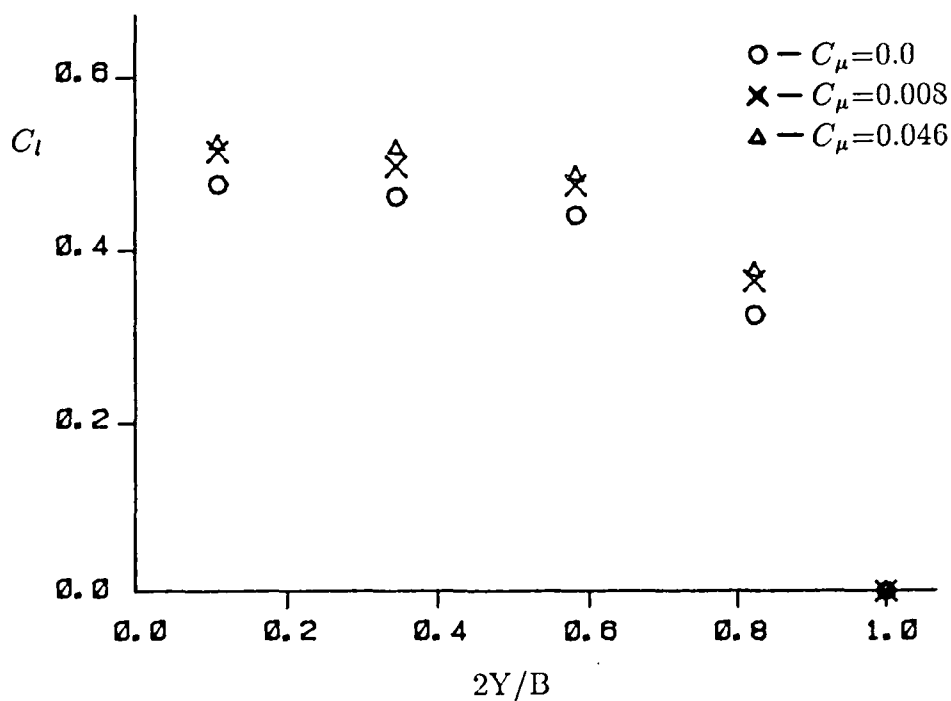Figure 3.7. Spanwise lift distribution for different C_μ, V_∞=20 m/s, α=5°, jet 1.

Figure 3.8. Spanwise lift distribution for different C_μ, V_∞=20 m/s, α=8°, jet 2.
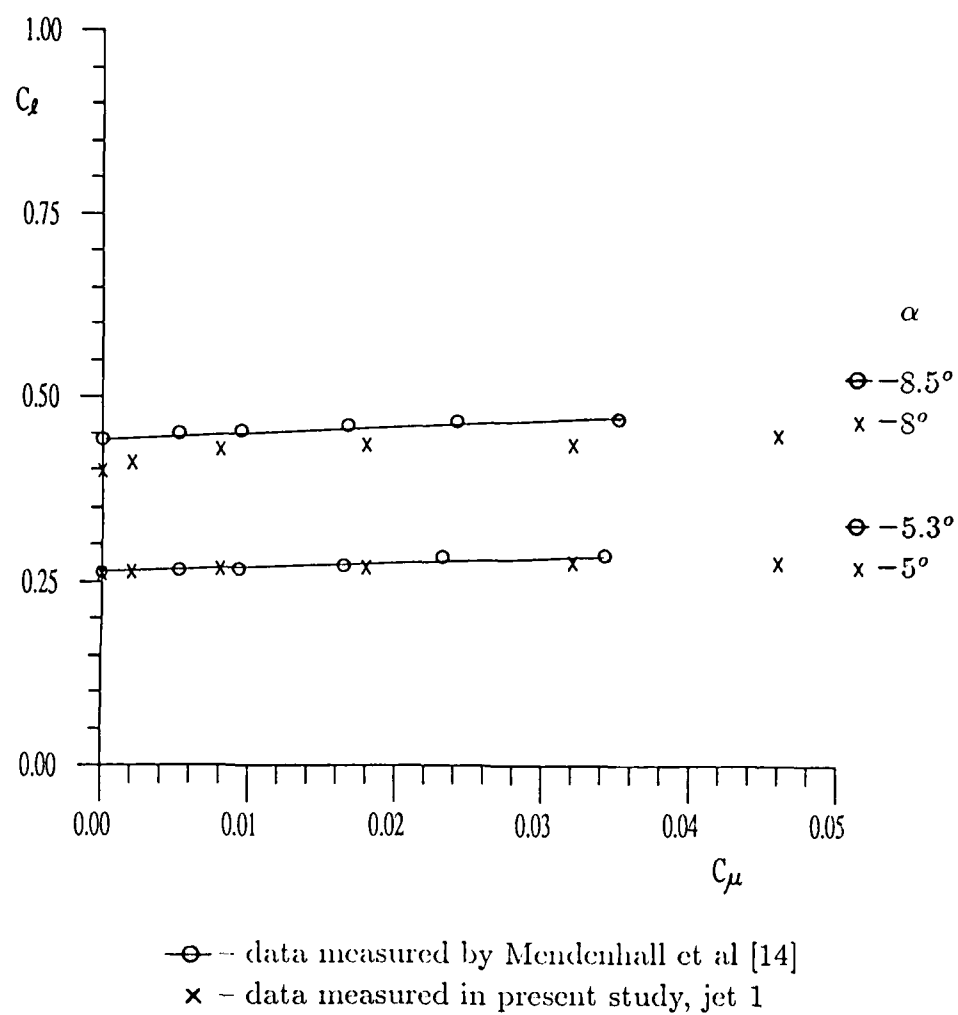
40

Fifure 3.9. Measured lift coefficients on wing.

IV. COMPUTATIONAL SIMULATIONS

From the flow visualization experiments conducted in the water tunnel, it was realized that flowfield generated by discrete jets blowing at the wingtip can be very complicated. In order to obtain knowledge on the trends of the parameters involved, a three dimensional vortex lattice method, in conjunction with some important physical assumptions, was developed and numerical simulation was performed. The simulated results were compared against experimental data and showed reasonable agreements.

4.1. MATHEMATICAL MODEL

As in the previous work [9], a single jet placed at the wingtip could be simulated as a turbulent symmetric jet stream effused into a uniform crossflow even though there was a upwash and the tip vortex flow formation around a finite span wing. In general, the jet spread, deformed, deflected and formed a pair of counter rotating vortices after leaving the exit. In turn, the jet interfered with the crossflow to create local blockage, entrainment and wake effect as well. With more jets, the problem of an individual wingtip jet was much more complicated than a single jet case, because in addition to the complications of a single jet, there were interactions among the jets themselves. Even though extensive studies have been made on a symmetric jet in a crossflow, the general prediction of flowfield was not completely satisfactory. Naturally for the multi-jets case, it was necessary to introduce some assumptions to reduce the complication of the problem to a level for mathematical modeling and subsequent computations.

In our case, since the main concern was not the jet itself but the effect of jets on the flows around the wing, we chose the simplest way to represent the jet with an approximate model. We extended the basic model for jet flow used in [9] to multi-jet case. The jet blowing from the tip was represented by a curved inviscid flow pipe. Following the Monical approach [22], the tube was assumed to have a square cross section with area equal to the area of the jet exit. The last segment of jet was assumed to be flared by considering the jet entrainment effect. The angle of flaring was determined based on the available empirical equation proposed by Monical. Margason [23] summarized previous studies and proposed

42

an empirical equation to represent the jet centerline trajectory. This empirical equation was used in this analysis.

For the multi-jets situation, each of the jets was modeled as a single one as described above. As an approximation in the present work, the interactions among the jets were embodied on the satisfaction of free slip surface boundary conditions on the jet tube but had no effect on the jet tube shape and trajectory.

4.2. PROCEDURE FOR SOLUTION

To be consistent with the approximation used in the jet simulation and the main interest of the problem, it was believed that the potential flow method would be appropriate. Under this model, the wing could be represented by a surface network of horseshoe vortices whose bound vortices coincide with constant percent chord lines along the wing surface by using the vortex lattice method. The free portions of vortices aft of the trailing edge were assumed to be parallel to the local flow. For simplicity, the wing wake and the tip vortex effects were ignored for the time being. The jet tubes were composed of a surface vortex network with the vortex lines as the lateral edge. The vortex networks were then attached to the tip of the main wing as schematically illustrated in Figure 4.1(a). What follows are the mathematical description and numerical solution of above model.

Let x, y, z be a cartesian coordinates in which x is parallel to the free stream, y is spanwise and normal to x axis, and z is normal to the x, y plane. Then for the cases of V_j/V_∞ greater than one, the centerline of jet can be described by the following equation, Margason [23], i.e.,

$$\frac{x - x_j}{d} = \frac{1}{4(V_j/V_\infty)^2 \sin^2 \delta_j} (\frac{y - y_j}{d})^3 - (\frac{y - y_j}{d}) \cot \delta_j$$

where x_j y_j are the coordinates of jet port center, d is the equivalent jet diameter, V_j is the jet efflux velocity and V_∞ is the freestream velocity, δ_j is the jet blowing angle with respect to the x axis. It was noted that the above equation was not fit to the case with a dihedral angle.

By using distribution of singularity to replace the wing and jet tube, the Laplace equation, which was the governing equation of a potential flow, was automatically satisfied

43
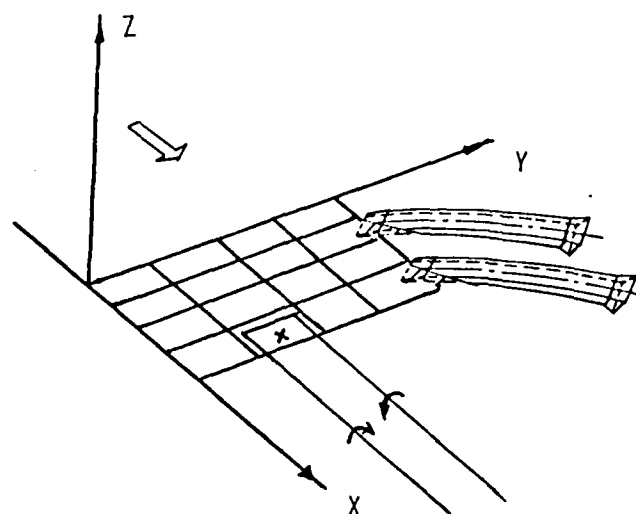
(a) Vortex Lattices Representation of
Wing With Jet Efflux Tube Attached.
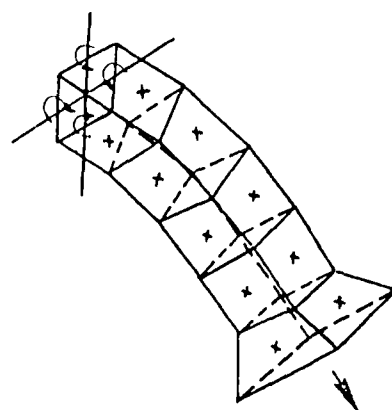
(b) Jet Efflux Tube Modeling

Figure 4.1. Schematic of analytical model

44

and the strength of the singularity was determined by applying corresponding no penetrable boundary condition. The control point for each panel of the main wing was located at three quarters of each local chord with individual elementary horseshoe vortices shedding from each surface element. The control points for vortex efflux tube were placed on the center of each elements of the network as shown in Figure 4.1(b). The flared end induced flow through the tube was calculated by the continuity consideration. The boundary condition was applied on every control point of each panel. It proved that the Kutta condition at the trailing edge of the wing was satisfied by selecting the position of each control point as described for the case without wingtip jets. Unfortunately, with jet flow, no such results exist.

Note that the wing was treated as a flat plate with the same planform as the wing here. If N is the number of elements on the wing surface, M is the number of jets and L is the number of elements on each side of the vortex tube, there are $N + 4 \times M \times L$ control points and this number of unknowns to represent the vortex strengths. By satisfying the boundary condition on each control point, the same number of equations as unknowns can be created. These were solved by direct inversion to avoid the divergence of iteration scheme due to the irregularity of the influence coefficients of the corresponding algebra equations.

After obtaining the vortex strength for each element, which represents the local aerodynamic load, the lift coefficient was calculated by integrating them on the wing.

4.3. COMPUTATIONAL RESULTS AND DISCUSSION

The analytical model as described above treated wingtip and wake flows with multi-jet blowing. Furthermore, the numerical simulation located the jet port at any position along the chordwise direction at the rectangular wing-tip, unlike test model, which only has three fixed ports available. For comparisons, the results from the classical lifting line theory [24], the numerical method and the measurement were plotted in Figure 4.2, which agree with each other reasonably. The results shown in Figure 4.3 are the optimization of single jet port location. It was found that the best position for a single jet blowing should
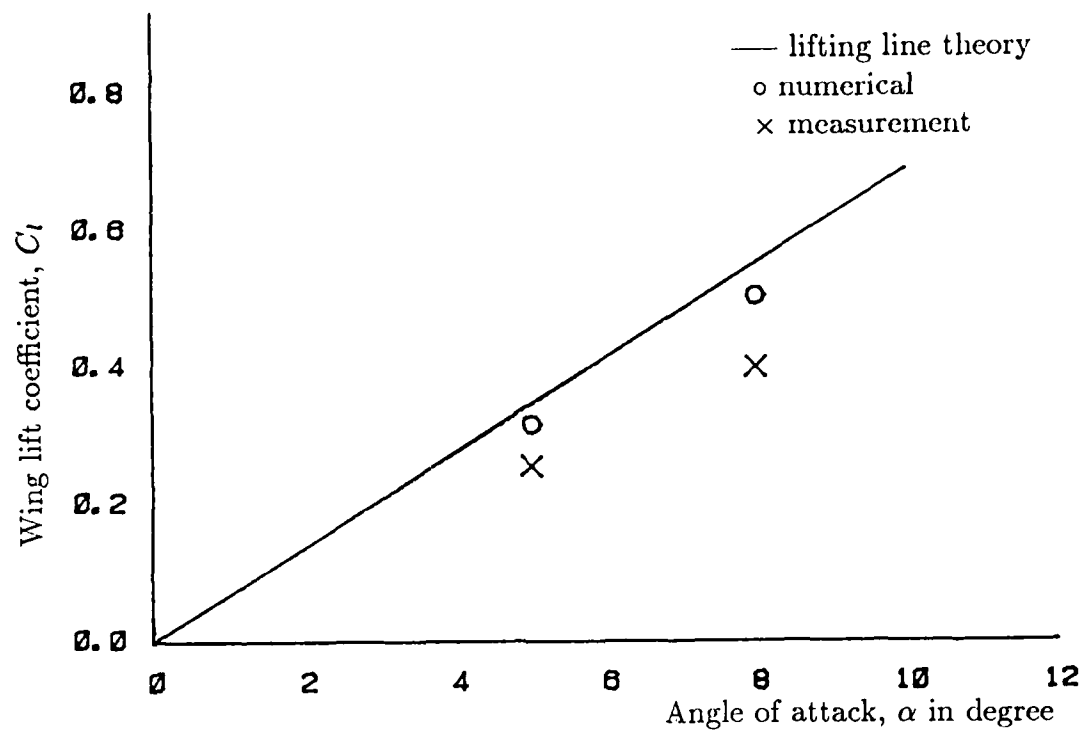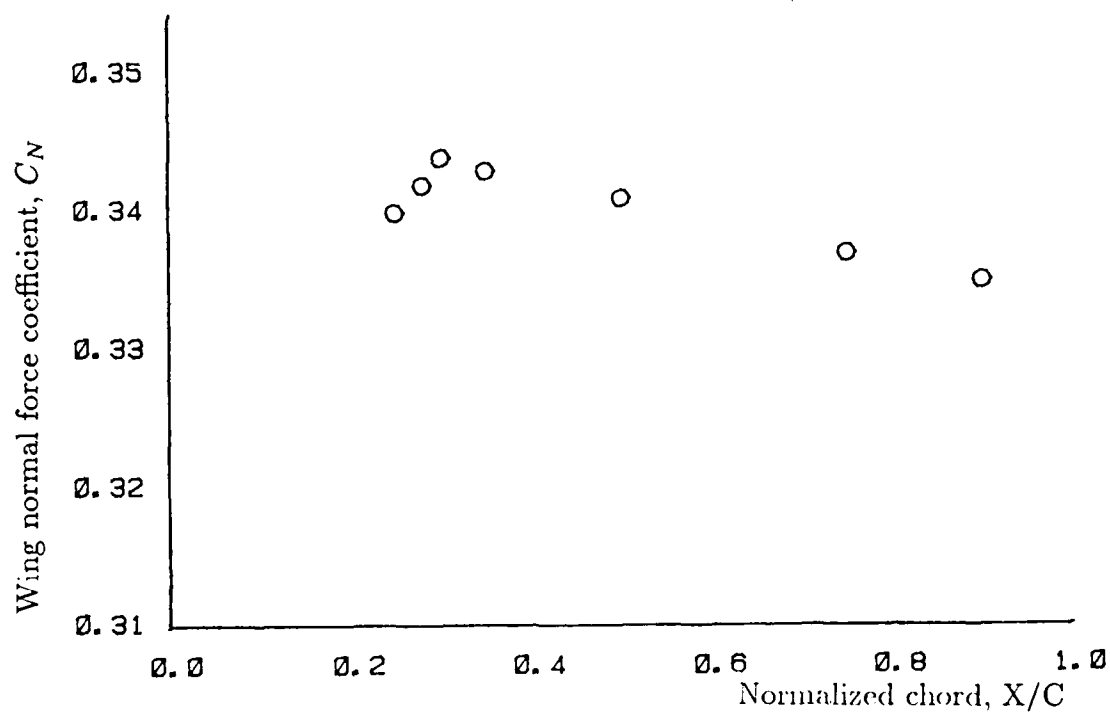
Figure 4.2. Comparison of basic wing lift coefficient

Figure 4.3. Optimization of jet port chordwise location

46

be located at about 30% of chordwise position, which is approximately the position of jet port 1 of the test model, thus agreed with the trend of results by the experiment.

From the above optimization analysis, the calculation with jet 1 was emphasized. The computed sectional loading with and without jet 1 are given in Figures 4.4 and 4.6. Comparisons of the total normal force argumentation with jet blowing are given in Figures 4.5 and 4.7. The agreement with data was good.

Similar results for multi-jets are shown in Figures 4.8 and 4.10 for the sectional load distribution with and without jets 1 and 2, at angles of attack 5° and 8°, respectively. Their lift argumentations were compared with measurements in Figures 4.9 and 4.11.

In spite of the simplified analytical model used in the computation, the comparison with measurements were generally encouraging.
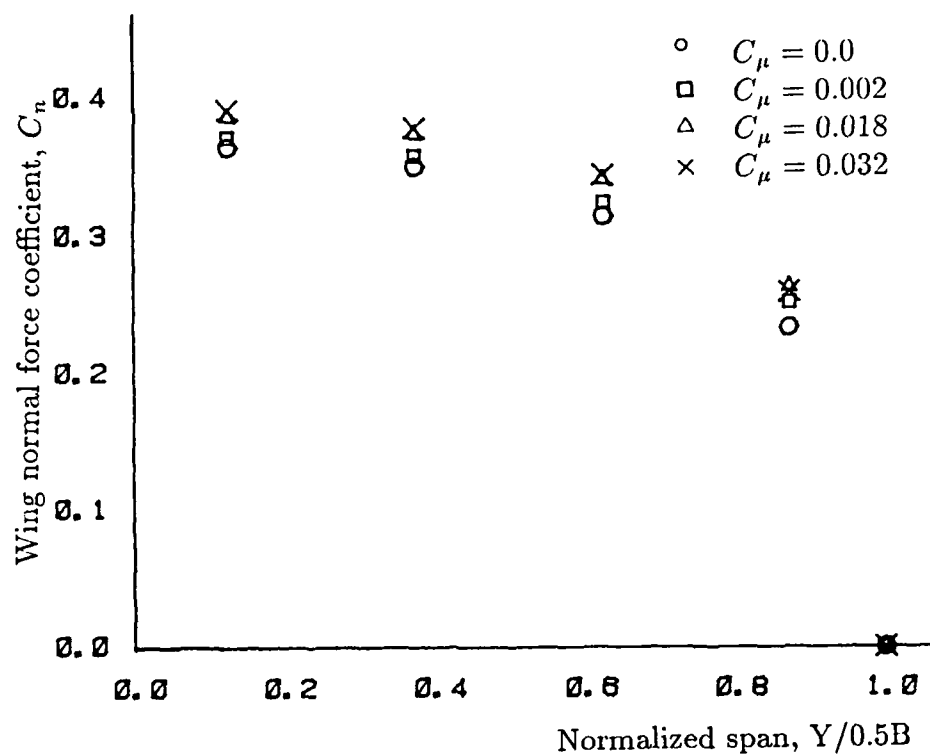
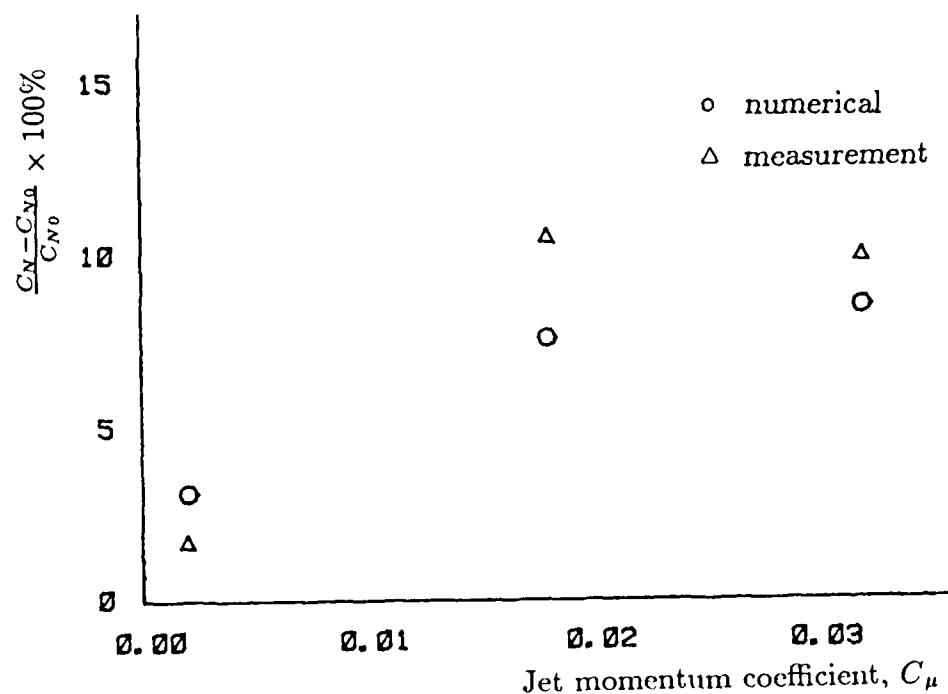Figure 4.4. Computed sectional load distribution (jet $\sharp$ 1, $\alpha = 5^0$)

Figure 4.5. Comparison of computed and measured results of total

normal force argumentation with jet blowing (jet $\sharp$ 1,$\alpha = 5^0$)

48

Figure 4.6. Computed sectional load distribution (jet $\sharp$ 1, $\alpha = 8^0$)

Figure 4.7. Comparison of computed and measured results of total

normal force argumentation with jet blowing (jet $\sharp$ 1, $\alpha = 8^0$)
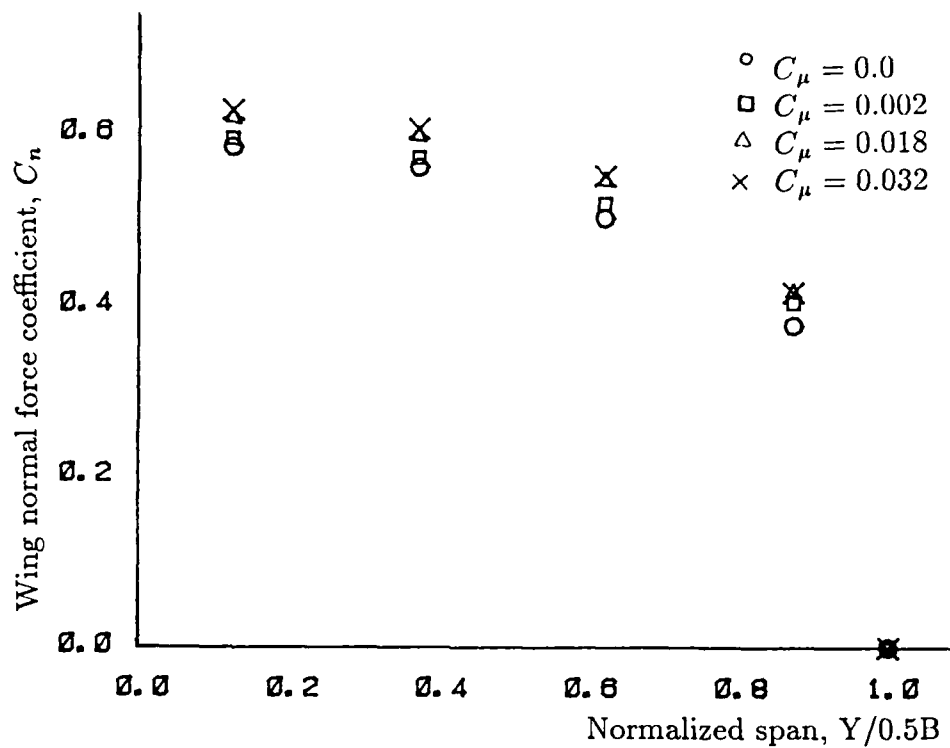
49

Figure 4.8. Computed sectional load distribution (jet ♮ 1 and ♮ 2, $\alpha = 5^0$)
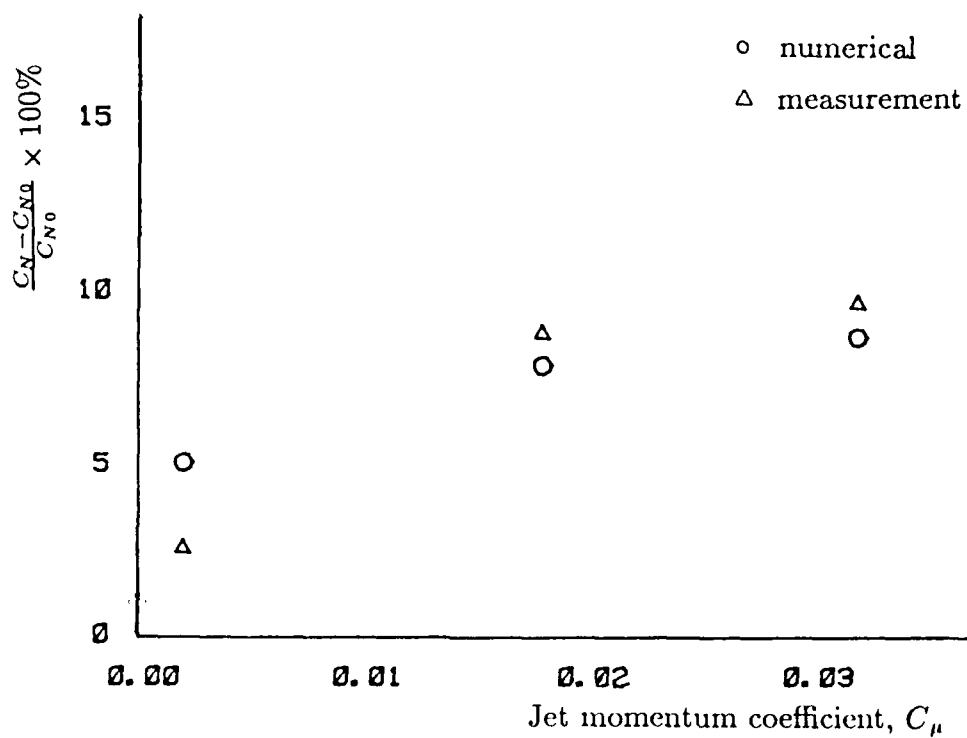

Figure 4.9. Comparison of computed and measured results of total normal force argumentation with jet blowing (jet ♮ 1 and ♮ 2 , $\alpha = 5^0$)
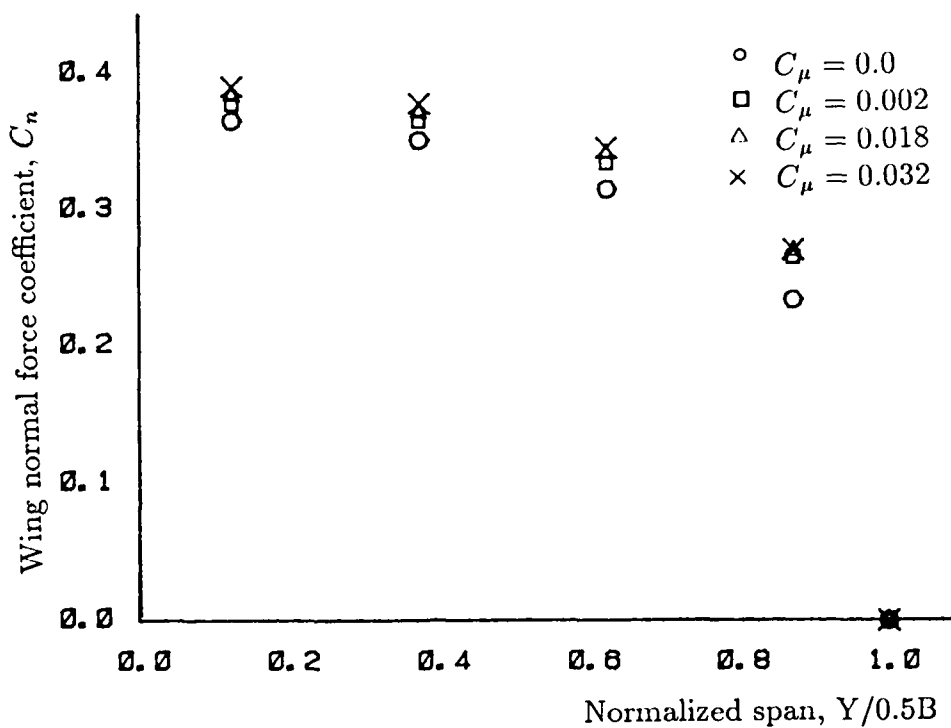
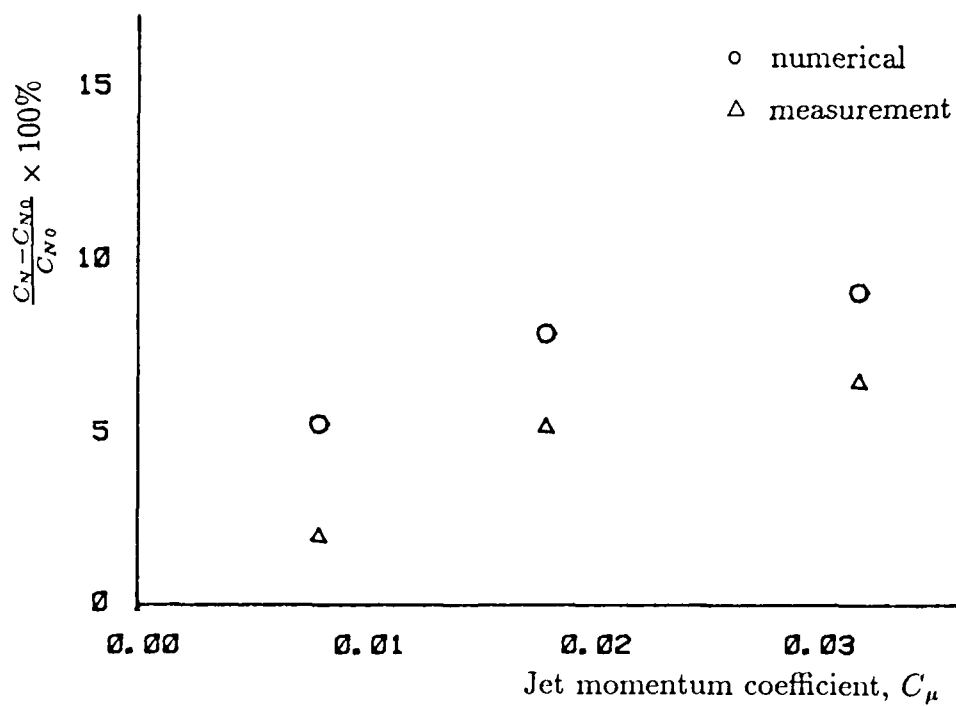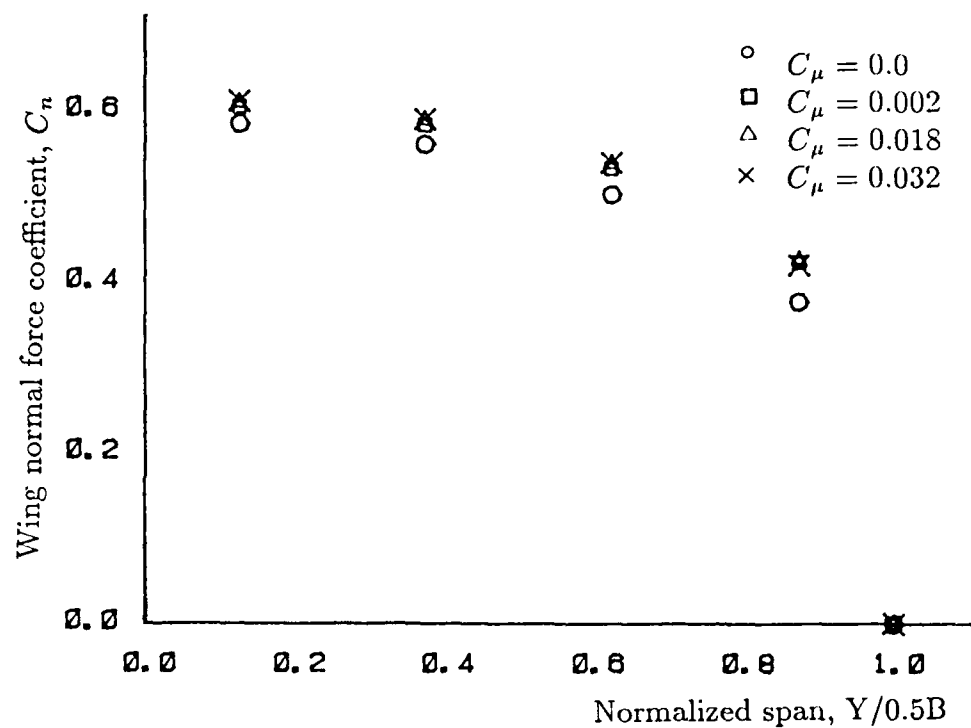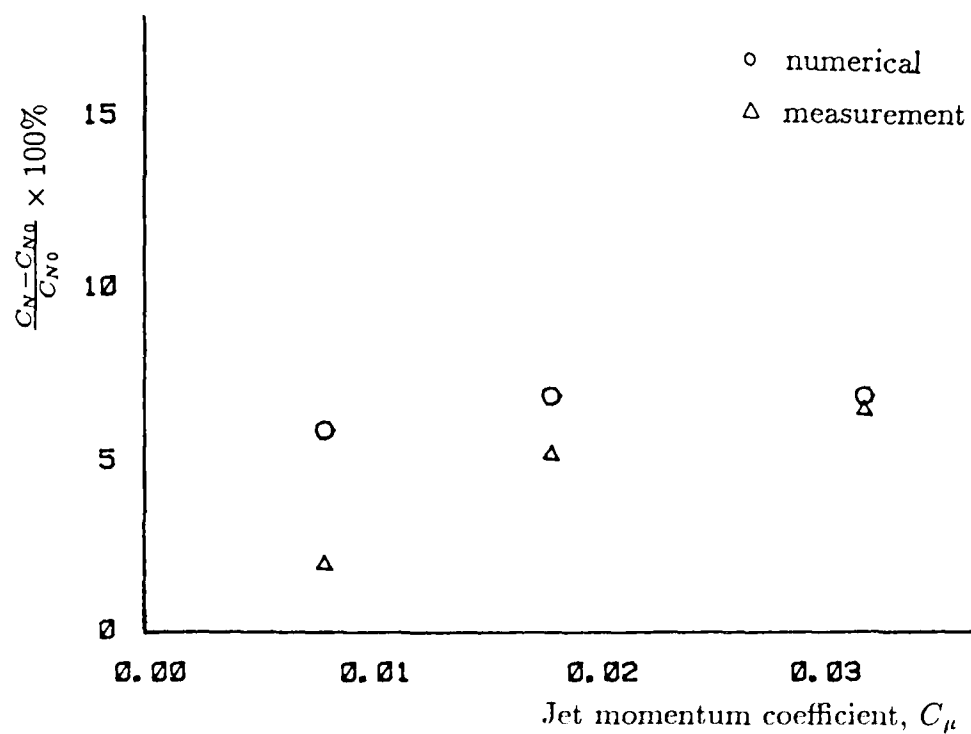Figure 4.10. Computed sectional load distribution (jet ♯ 1 and ♯ 2, $\alpha = 8^0$)

Figure 4.11. Comparison of computed and measured results of total normal force argumentation with jet blowing (jet ♯ 1 and ♯ 2 , $\alpha = 8^0$)

V. CONCLUSION

A study of discrete wingtip jets has been conducted. This study consisted of careful flow visualization in water tunnel and wind tunnel, detail pressure measurement in the wind tunnel and computations based on a simplified analytical model. The following conclusions were been drawn:

1. The roll-up wing-tip vortex could be dispersed significantly by the wingtip jets. More jets with higher blowing coefficients resulted in a better dispersion.

2. The dispersed wingtip wake flow contained many different types of vortices.

3. Flow pattern of a single jet on wingtip were similar to the flowfield of a rectangular cross section jet issued from a flat plat asymmetric to uniform crossflow. All the vortices observed for the jet in uniform crossflow were identified for the wingtip jet flow.

4. Pressure distribution on the wing was improved by the wingtip jets. The entire wing flow is influenced with the wingtip incremental gain being large and it tapered-off to a small gain at the root.

5. The simplified analytical numerical model simulation of the wingtip jet flow agreed reasonably well with the experimental observations and thus can be useful as a first step design tool.

6. Flow in the wingtip region is three dimensional and with tip jets represent certain unsteadiness. Further studies in this area should be concerned with the unsteady and viscous effects.

VI. REFERENCE

1. Ayers, R. F. and Wilde, M. R., " An experimental investigation of the aerodynamic characteristics of a low aspect ratio swept wing with blowing in a spanwise direction from the tips," The College of Aeronautics, Cranfield, UK Note 57, September 1956.

2. Lloyd, A., "The effects of spanwise blowing on the aerodynamic characteristics of a low aspect ratio wing," Von Karman Institute Project Report 1963-90. Rhode-st. Geneses, Belgium, 1963.

3. White, H. E., "Wind tunnel investigation of the use of wing-tip blowing to reduce drag for take-off and landing," The David Taylor Model Basin Aerodynamics Laboratory, AERO Report 1040, January 1963.

4. Carafoli, F. and Camarasescu, N., "New researchers on small span-chord ratio wings with lateral jets," AD-733858, FTDHC 23-319-71, October 1971.

5. Wu, J. M., Vakili, A. D. and Chen, Z. L., "Wing-tip jets aerodynamic performance," Proceedings of the 13 International Council for Aeronautical Sciences, Ed. B. Laschka and R. Staufenbiel, Seattle, Washington, August 1982.

6. Briggs, M. M., and Schwind, R. G., "Augmentation of fighter aircraft lift and STOL capability by blowing outboard from the wing tips," AIAA Paper 83-0078, January 1983.

7. Wu, J. M., Vakili, A. D., Chen, Z. L. and Gilliam, F. T., "Investigation on the effects of discrete wingtip jets," AIAA Paper 83-0546, January 1983.

8. Gilliam, F. T.,"An investigation of the effects of discrete wing tip jets on wake vortex roll up," Ph. D. dissertation, The University of Tennessee Space Institute, August 1983.

9. Wu, J. M. and Vakili, A. D., "Aerodynamic improvements by discrete wing tip jets," AFWAL-TR-84-3009. March 1984.

10. Wu, J. M., Vakili, A. D., Gilliam, F. T., "Aerodynamic interaction of wing tip flow with discrete wing tip jets," AIAA Paper 84-2206, August 1984.

11. Tavella, D. A., Wood, N. J., and Harrits, P., "Influence of the tip blowing on rectangular wings," AIAA Paper 85-5001, October 1985.

12. Tavella, D. A., Lee, C. S., and Wood, N. J., "Influence of wing tip configuration on lateral blowing efficiency," AIAA Paper 86-0475, January 1986.

13. Lee, C. S., Tavella, D. A., Wood, N. J., and Roberts, L., "Flow structure of lateral wing tip blowing," AIAA Paper 86-1810, June 1986.

14. Mendenhall, M. R., Caruso, S. C., Lesieutre, D. J. and Childs, R. E., " An investigation of wing lift augmentation with spanwise tip blowing," AFWAL-86-3112, Nielsen Engineering & Research, Inc. April 1987.

15. Lee, C. S., Tavella, D. A. and Wood, N. J., "Flow structure and scaling in lateral wing-tip blowing," Stanford University, August 1987.

16. Carafoli, E. and Camarasescu, N., "New research on small span-chord ratio wings with lateral jets," *Sutdii si Cercetari de Mecanica Aplicata*, Vol 29, No. 4, pp. 947-962, 1970. Available in English as Translation FTD-HC-23-319, Foreign Technology Division, Air Force Station Command, October 1971.

17. Chen, Z. L. and Wu, J. M., "Jet wing vortex lattice theory with nonlinear wake and tip flow," AIAA Paper 83-0263, January 1983.

18. Tavella, D. A. and Roberts, L., "The concept of lateral blowing," AIAA Paper 85-5001, October 1985.

19. Wu, J. M., Vakili, A. D., and Yu, F. M., "Investigation of the interacting flow of non-symmetric jets in cross flow," AIAA Paper 86-0280, January 1986.

20. Wu, J. M., Vakili, A. D., and Yu, F. M., "Investigation of non-symmetric jets in cross flow," AFOSR Contract Report AFOSR-84-0114, December 1986.

21. Yu, F. M., Wu, J. M. and Vakili, A. D., "Investigation of vortical flow properties of jet in cross flow," AIAA Paper 88-0698, January 1988.

22. Monical, R. E., "A method of representing fan-wing combination for 3-D potential solution," J. of Aircraft, Vol. 2, No. 6, 1965.

23. Margason, R. J., "The path of a jet directed at large angle to a subsonic free stream," NASA TND-4919, 1968.

24. Millikan, C. B., "Aerodynamics of the airplane", GALCIT Aeronautical Series, John Wiley & Sons, 1941.